LIMITING EXIT LOCATION DISTRIBUTIONS IN THE STOCHASTIC EXIT PROBLEM

ROBERT S. MAIER* AND DANIEL L. STEIN†

Abstract. Consider a two-dimensional continuous-time dynamical system, with an attracting fixed point S. If the deterministic dynamics are perturbed by white noise (random perturbations) of strength ϵ, the system state will eventually leave the domain of attraction Ω of S. We analyse the case when, as $\epsilon \to 0$, the exit location on the boundary $\partial\Omega$ is increasingly concentrated near a saddle point H of the deterministic dynamics. We show using formal methods that the asymptotic form of the exit location distribution on $\partial\Omega$ is generically non-Gaussian and asymmetric, and classify the possible limiting distributions. A key role is played by a parameter μ, equal to the ratio $|\lambda_s(H)|/\lambda_u(H)$ of the stable and unstable eigenvalues of the linearized deterministic flow at H. If $\mu < 1$ then the exit location distribution is generically asymptotic as $\epsilon \to 0$ to a Weibull distribution with shape parameter $2/\mu$, on the $\mathcal{O}(\epsilon^{\mu/2})$ lengthscale near H. If $\mu > 1$ it is generically asymptotic to a distribution on the $\mathcal{O}(\epsilon^{1/2})$ lengthscale, whose moments we compute. Our treatment employs both matched asymptotic expansions and stochastic analysis. As a byproduct of our treatment, we clarify the limitations of the traditional Eyring formula for the weak-noise exit time asymptotics.

Key words. Stochastic exit problem, large fluctuations, large deviations, Wentzell-Freidlin theory, exit location, saddle point avoidance, first passage time, matched asymptotic expansions, singular perturbation theory, stochastic analysis, Ackerberg-O'Malley resonance.

AMS subject classifications. 60J60, 35B25, 34E20

1. Introduction. We consider the problem of noise-activated escape from a planar domain Ω with smooth boundary, in the limit of weak noise. If $\boldsymbol{b} = (b^i)$, $i = 1,2$ is a smooth vector field on a neighborhood of the closure $\bar{\Omega}$, we define the random process $\boldsymbol{x}_\epsilon(t) = (x^i_\epsilon(t))$, $i = 1,2$ by the Itô stochastic differential equation

$$dx^i_\epsilon(t) = b^i(\boldsymbol{x}_\epsilon(t))\,dt + \epsilon^{1/2}\sum_\alpha \sigma^i{}_\alpha(\boldsymbol{x}_\epsilon(t))\,dw_\alpha(t) \tag{1.1}$$

and an appropriate initial condition. Here $w_\alpha(t)$, $\alpha = 1,2$, are independent Wiener processes and $\sigma = (\sigma^i{}_\alpha)$ is a 2-by-2 noise matrix, like $\boldsymbol{b}$ a function of position $\boldsymbol{x} = (x^i)$, $i = 1,2$. The associated diffusion tensor $\boldsymbol{D} = (D^{ij})$ is defined by

$$D^{ij} = \sum_\alpha \sigma^i{}_\alpha \sigma^j{}_\alpha, \tag{1.2}$$

i.e., $\boldsymbol{D} = \sigma\sigma^T$. We assume strict ellipticity, *i.e.*, that $\boldsymbol{D}$ is nonsingular on Ω and its boundary, and that its $\boldsymbol{x}$-dependence is smooth on a neighborhood of $\bar{\Omega}$. $\epsilon > 0$ is a noise strength parameter. The subscripts on x^i_ϵ and $\boldsymbol{x}_\epsilon$ emphasize the ϵ-dependence of the random process, which may be viewed as a dynamical system stochastically perturbed by noise.

Of interest in applications is the case when Ω contains only a single stable fixed point S of the drift field $\boldsymbol{b}$, and S serves as an attractor for the whole of Ω. If Ω is the entire domain of attraction of S, the boundary $\partial\Omega$ will not be attracted to S: it will be a separatrix between domains of attraction. This 'characteristic boundary case' is particularly important and difficult to study. We shall restrict ourselves to this case, assuming that $\partial\Omega$ is a smooth characteristic curve of $\boldsymbol{b}$ containing fixed points (alternating saddle points and unstable fixed points, as in

*Dept. of Mathematics, University of Arizona, Tucson, AZ 85721, USA. Partially supported by the National Science Foundation under grants NCR-90-16211 and DMS-95-00792. E-mail: rsm@math.arizona.edu.

†Dept. of Physics, University of Arizona, Tucson, AZ 85721, USA. Partially supported by the Department of Energy under contract DE-FG03-93ER25155. E-mail: dls@physics.arizona.edu.

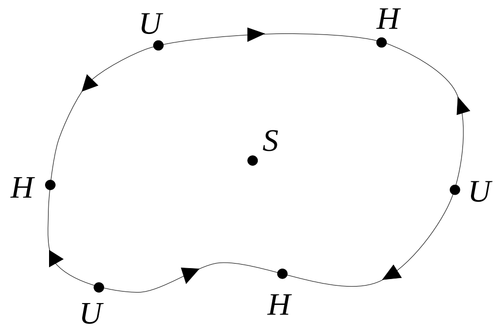

FIG. 1.1. *The structure of the drift field* $\boldsymbol{b}$ *on* Ω*, when* Ω *is bounded. The boundary* $\partial\Omega$*, being a separatrix, is not attracted to the stable fixed point* S*, though all points in* Ω *are attracted to* S*. Saddle points* (H) *and unstable fixed points* (U) *alternate around the boundary.*

Fig. 1.1). We allow Ω to be unbounded. If the initial condition is $\boldsymbol{x}_\epsilon(0) = S$ and τ_ϵ is the first passage time from S to the boundary (*i.e.*, the first exit time), we shall study the behavior of the exit location distribution $p_\epsilon(\boldsymbol{x})\, d\boldsymbol{x} \stackrel{\text{def}}{=} \Pr\{\boldsymbol{x}_\epsilon(\tau_\epsilon) \in \boldsymbol{x} + d\boldsymbol{x}\}$ on $\partial\Omega$ in the $\epsilon \to 0$ limit, and the small-ϵ asymptotics of the mean first passage time (MFPT) $E\tau_\epsilon$.

Exit problems of this sort, in more than one dimension, have a long history [42]. They arose originally in chemical physics [2, 4, 8, 24], but occur in other fields of physics [41, 51] as well as in systems engineering [31, 52] and theoretical ecology [29, 36, 37]. In recent years two different approaches have been used: rigorous large deviations theory [9, 10, 19, 20] and formal but systematic asymptotic expansions [29, 39, 42, 50]. The rigorous approach yields comparatively weak but still very useful results. In particular much light is thrown on exit problems by the Wentzell-Freidlin quasipotential [20], or classical action function, $W : \bar{\Omega} \to \mathbb{R}^+$. $W(\boldsymbol{x})$ is best thought of as a measure of how difficult it is for the process $\boldsymbol{x}_\epsilon(t)$ to reach the point $\boldsymbol{x}$; as $\epsilon \to 0$ the frequency of excursions to the vicinity of $\boldsymbol{x}$ will be suppressed exponentially, with rate constant $W(\boldsymbol{x})$. $W(\boldsymbol{x})$ can be computed from the 'classical' trajectory extending from S to $\boldsymbol{x}$, *i.e.*, the most probable (as $\epsilon \to 0$) fluctuational path from S to $\boldsymbol{x}$ [29, 34].

Normally one expects that W will attain a minimum on $\partial\Omega$ at one of the saddle points. This can be shown to imply that as $\epsilon \to 0$, the exit location on $\partial\Omega$ converges in probability to the saddle point. Actually the behavior of W on $\partial\Omega$, and its consequences, are not yet fully understood. (For some partial results on the smoothness of W, see Day and Darden [14] and Day [13].) Recent treatments [11, 32] indicate that as $\epsilon \to 0$ it is possible for the exit location to converge to an *unstable* fixed point on $\partial\Omega$, due to local constancy of W on the boundary. In this paper we consider only models displaying the conventional behavior: as $\epsilon \to 0$ the exit location should converge to some distinguished saddle point H on $\partial\Omega$, due to W on $\partial\Omega$ having a unique global minimum at H.

Much previous work, in particular on physical applications, has dealt with a special case: when the mean drift b^i equals $-D^{ij}\partial_j\Phi$, for some smooth potential function Φ. (Here $\partial_j \stackrel{\text{def}}{=} \partial/\partial x^j$; summation over repeated Roman indices is assumed henceforth.) In this case the point H will simply be a saddle point of Φ. This gradient (or 'conservative') case finds many applications in physics, but from a mathematical point of view is highly nongeneric. W can be solved for exactly (it equals 2Φ), and one can show formally that in the limit of weak noise the distribution of the exit location on $\partial\Omega$ is asymptotic to a Gaussian centered on H, with $\mathcal{O}(\epsilon^{1/2})$ standard deviation.

It has been known for some time that the exit location distribution in nongradient models tends to be *skewed*. What is meant by this is that as $\epsilon \to 0$, the exit location converges to H but its distribution $p_\epsilon(\boldsymbol{x})\,d\boldsymbol{x}$ on $\partial\Omega$ fails, due to a lack of symmetry, to be asymptotic to a Gaussian centered on H. Skewing was discovered by Bobrovsky and Schuss [6]; for recent work, see Bobrovsky and Zeitouni [7], Day [12], and Ryter and Bobrovsky [45]. Also, skewed limiting exit location distributions have been computed explicitly by the authors [33]. We show in this paper, using formal methods, that skewing is a generic phenomenon. Our results on genericity supplement the rigorous results of Bobrovsky and Zeitouni, and of Day. We also derive a general result, analogous to the central limit theorem, which characterizes skewing: *As $\epsilon \to 0$, in any generic stochastic exit model (with characteristic boundary) of the above sort, the exit location distribution, on an appropriate ϵ-dependent lengthscale near H, will be asymptotic to a non-Gaussian distribution that belongs to one of two well-defined classes.* Which limiting distribution occurs is largely determined by the behavior of the model near H (*i.e.*, the ratio $\mu \stackrel{\text{def}}{=} |\lambda_s(H)|/\lambda_u(H)$ of the stable and unstable eigenvalues of the linearization of $\boldsymbol{b}$ at H, which we assume to be nonsingular). One of the two classes is the class of Weibull distributions, which are familiar from statistics [3]. The asymptotic exit location distributions in the second class are more complicated, and we do not derive explicit expressions for them in this paper. We do however provide an algorithm for computing their moments, in terms of the correlation functions of a conditioned three-dimensional Bessel process.

That generic drift fields give rise to non-Gaussian asymptotic exit location distributions is slightly surprising from the point of view of large deviations theory. One might expect that on $\partial\Omega$, W in general attains a quadratic minimum at H. If $\partial^2 W/\partial s^2(s=0)$ equals σ^{-2} (s being the arc length along $\partial\Omega$, measured from H), the abovementioned exponential suppression as $\epsilon \to 0$ would presumably give rise to a factor $\exp(-s^2/2\sigma^2\epsilon)$ in the exit location density $p_\epsilon(s)$. This is precisely a Gaussian centered on H, on the $\mathcal{O}(\epsilon^{1/2})$ lengthscale. The generic case would therefore seem to resemble the gradient case.

It is tempting to ascribe the discrepancy between this prediction and the phenomenon of skewing to what theoretical physicists would call a 'prefactor effect', *i.e.*, the presence of subdominant (as $\epsilon \to 0$) terms in the exit location density that are not included in the comparatively coarse asymptotics supplied by large deviations theory. However, this is not the case. The prediction assumed that if W has a minimum at H, it has a quadratic minimum there. It turns out that generically, W is not even twice differentiable at H; in fact, $\partial^2 W/\partial s^2$ is generically discontinuous at $s = 0$. This discontinuity causes the exit location density $p_\epsilon(s)$, even if (in the small-ϵ limit) it is localized on the $\mathcal{O}(\epsilon^{1/2})$ lengthscale near H, to have different Gaussian falloff rates as $s/\epsilon^{1/2} \to +\infty$ and $s/\epsilon^{1/2} \to -\infty$. This gives rise to skewing. The abovementioned limiting Weibull distributions, which are one-sided, arise when either $\partial^2 W/\partial s^2(0+)$ or $\partial^2 W/\partial s^2(0-)$ equals zero (a generic occurrence, when $\mu < 1$); on account of the corresponding zero Gaussian falloff rate, they are localized on a larger lengthscale than $\mathcal{O}(\epsilon^{1/2})$. That skewing is generic in models with $\mu < 1$ was shown rigorously by Bobrovsky and Zeitouni [7] and Day [12], but the appropriate lengthscale was unclear. Our analysis reveals that $\mathcal{O}(\epsilon^{\mu/2})$ is the lengthscale on which the exit location distribution is supported.

In Section 4, which is the linchpin of this paper, we give a simple *geometric* explanation of the generic discontinuity in $\partial^2 W/\partial s^2$ at $s = 0$. The discontinuity occurs both when $\mu < 1$ and when $\mu > 1$. The reader may wish to glance ahead at Fig. 4.2, which shows the generic behavior of the classical trajectories giving rise to $W(\boldsymbol{x})$, for $\boldsymbol{x}$ in the vicinity of H. There is a wedge-shaped 'classically forbidden' region emanating from H, which is reached only by piecewise smooth (rather than smooth) classical trajectories. This region includes all the boundary points to one side of H, but not the other. This asymmetry is the ultimate source of the skewing phenomenon.

A byproduct of our analysis of skewing is an increased understanding of the limitations of the classical ('Eyring') formula for the weak-noise MFPT asymptotics [27, 42, 46, 50]. Although this formula has been widely used, we shall show that it is valid, without qualification, only when the classically forbidden wedge is absent.

2. Matched asymptotic expansions. We now begin our analysis. The random process $\boldsymbol{x}_\epsilon(t)$, $t \geq 0$ has generator

$$\mathcal{L}_\epsilon = -(\epsilon/2) D^{ij} \partial_i \partial_j - b^i \partial_i. \tag{2.1}$$

The formal adjoint $\mathcal{L}_\epsilon^*$ of $\mathcal{L}_\epsilon$ is defined by

$$\mathcal{L}_\epsilon^* \rho = -(\epsilon/2) \partial_i \partial_j [D^{ij} \rho] + \partial_i [b^i \rho]. \tag{2.2}$$

The density $\rho(\boldsymbol{x}, t)$ of the probability distribution $\rho(\boldsymbol{x}, t)\, d\boldsymbol{x} \stackrel{\text{def}}{=} \Pr\{\boldsymbol{x}_\epsilon(t) \in \boldsymbol{x} + d\boldsymbol{x}\}$ will satisfy $\dot{\rho} = -\mathcal{L}_\epsilon^* \rho$, the forward Kolmogorov (or Fokker-Planck) equation. So the spectral theory of the operators $\mathcal{L}_\epsilon$ and $\mathcal{L}_\epsilon^*$ is relevant to the stochastic exit problem. If they are equipped with Dirichlet (absorbing) boundary conditions on $\partial\Omega$ and Ω is bounded, it follows by standard methods [23] that they have pure point spectrum, with smooth eigenfunctions, and that the principal eigenvalues of $\mathcal{L}_\epsilon$ and $\mathcal{L}_\epsilon^*$ (the ones with minimum real part) are real. Also, the corresponding principal eigenfunctions may be taken to be real and positive on Ω. If Ω is unbounded we assume these properties continue to hold; they will hold if the stochastic model is sufficiently stable at infinity.

It is well known that the weak-noise ($\epsilon \to 0$) asymptotics of the stochastic exit problem are determined by the *quasistationary density*, *i.e.*, the principal eigenfunction v_ϵ^0 of $\mathcal{L}_\epsilon^*$. That is because it is the slowest decaying eigenmode. Its eigenvalue $\lambda_\epsilon^{(0)}$, which is guaranteed to be real, may be viewed as the rate at which the mode is absorbed on $\partial\Omega$. This rate will decrease to zero exponentially as $\epsilon \to 0$. Since (up to exponentially small relative errors) $E\tau_\epsilon \sim \left(\lambda_\epsilon^{(0)}\right)^{-1}$, $\epsilon \to 0$, the MFPT will grow exponentially in the weak-noise limit.

The $\epsilon \to 0$ asymptotics of the density p_ϵ of the exit location measure on $\partial\Omega$ may be written

$$p_\epsilon(\boldsymbol{x}) \propto n_i(\boldsymbol{x}) \partial_j [D^{ij} v_\epsilon^0](\boldsymbol{x}), \qquad \epsilon \to 0, \tag{2.3}$$

where $n_i(\boldsymbol{x})$ is the outward normal to $\partial\Omega$ at $\boldsymbol{x}$. The constant of proportionality here is fixed by the normalization condition

$$\int_{\boldsymbol{x} \in \Omega} p_\epsilon(\boldsymbol{x})\, d\boldsymbol{x} = 1. \tag{2.4}$$

Equation (2.3) simply says that p_ϵ is asymptotic to the absorption location density of the eigenmode v_ϵ^0 on $\partial\Omega$, as $\epsilon \to 0$.

If J_0^i is the probability current arising from v_0^ϵ, *i.e.*,

$$J_0^i = -(\epsilon/2) \partial_j [D^{ij} v_\epsilon^0] + b_i v_\epsilon^0 \tag{2.5}$$

then on account of the interpretation of $\lambda_\epsilon^{(0)}$ as an absorption rate,

$$\lambda_\epsilon^{(0)} = \int_{\boldsymbol{x} \in \partial\Omega} J_0^i(\boldsymbol{x}) n_i(\boldsymbol{x})\, d\boldsymbol{x}, \tag{2.6}$$

provided that v_ϵ^0 is normalized to total unit mass. If this normalization condition does not hold, (2.6) must be replaced by

$$\lambda_\epsilon^{(0)} = \frac{\int_{\boldsymbol{x}\in\partial\Omega} J_0^i(\boldsymbol{x}) n_i(\boldsymbol{x})\, d\boldsymbol{x}}{\int_{\boldsymbol{x}\in\Omega} v_\epsilon^0(\boldsymbol{x})\, d\boldsymbol{x}}. \tag{2.7}$$

In any event, the weak-noise asymptotics of the MFPT are determined by the asymptotics of v_ϵ^0.

We shall employ a now standard method of matched asymptotic expansions [32, 33, 34, 42] to approximate v_ϵ^0 as $\epsilon \to 0$, and use (2.3) and (2.7) to compute the asymptotics of p_ϵ and $\lambda_\epsilon^{(0)}$. Our treatment is facilitated by the fact that $\lambda_\epsilon^{(0)} \to \lambda_0^{(0)} = 0$ exponentially rapidly; up to exponentially small relative errors, it suffices when approximating v_ϵ^0 in various regions of Ω to view it as a solution of $\mathcal{L}_\epsilon^* v_\epsilon^0 = 0$, rather than of $\mathcal{L}_\epsilon^* v_\epsilon^0 = \lambda_\epsilon^{(0)} v_\epsilon^0$.

We shall approximate in the following three asymptotic regions. Recall that we are considering the case when W attains a global minimum on $\partial\Omega$ at a saddle point H, and H is the limiting exit location.

1. The body of Ω: a region including all of Ω except the local region near S, and the boundary layer of width $\mathcal{O}(\epsilon^{1/2})$ near the characteristic boundary $\partial\Omega$. This region contains the fluctuational paths from the vicinity of the stable point S to the vicinity of H.
2. A local (stable) region of size $\mathcal{O}(\epsilon^{1/2})$ centered on the stable point S.
3. A boundary region, of size as yet unspecified but centered on H, and lying within the boundary layer of width $\mathcal{O}(\epsilon^{1/2})$.

In Section 3 we shall construct an ‘outer’ approximation to v_ϵ^0, valid in the body of Ω. After discussing its geometric aspects, in Section 4 we shall analyse geometrically the small-ϵ behavior of v_ϵ^0 in the other two regions.

3. The outer approximation and Lagrangian geometry. The appropriate outer approximation to the quasistationary density v_ϵ^0 is a WKB expansion; equivalently, a characteristic (ray) expansion. We write

$$v_\epsilon^0(\boldsymbol{x}) \sim K(\boldsymbol{x}) \exp\left(-W(\boldsymbol{x})/\epsilon\right), \qquad \epsilon \to 0, \tag{3.1}$$

for certain functions $W : \bar{\Omega} \to \mathbb{R}$ and $K : \bar{\Omega} \to \mathbb{R}$ normalized so that $W(S) = 0$ and $K(S) = 1$, whose smoothness properties are as yet unspecified. We could instead attempt an approximation of higher order, with $K(\boldsymbol{x})$ in (3.1) replaced by $K_0(\boldsymbol{x}) + \epsilon K_1(\boldsymbol{x}) + \cdots$. However, we shall see in Section 8 that there may be difficulties with matching such outer expansions (in integer powers of ϵ) to the inner approximation in the boundary region.

Substituting the approximation (3.1) into the approximate forward Kolmogorov equation $\mathcal{L}_\epsilon^* v_\epsilon^0 = 0$, and collating the coefficients of powers of ϵ, yields equations for W and K:

$$H(x^i, \partial_i W) = 0 \tag{3.2a}$$

$$\begin{aligned} &\left[\frac{\partial H}{\partial p^i}(x^i, \partial_i W)\right] \partial_i K = \\ &-\left[\frac{\partial^2 H}{\partial x^i \partial p_i}(x^i, \partial_i W) + \frac{1}{2}\frac{\partial^2 W}{\partial x^i \partial x^j}(\boldsymbol{x})\frac{\partial^2 H}{\partial p_i \partial p_j}(x^i, \partial_i W)\right] K. \end{aligned} \tag{3.2b}$$

Here $H : \bar{\Omega} \times \mathbb{R}^2 \to \mathbb{R}$ is the Hamiltonian (or energy) function

$$H(x^i, p_i) = \frac{1}{2} D^{ij}(\boldsymbol{x}) p_i p_j + b^i(\boldsymbol{x}) p_i, \tag{3.3}$$

and the eikonal equation (3.2a) is the corresponding zero-energy Hamilton-Jacobi equation. For consistency, we have also used this Hamiltonian in the transport equation (3.2b). The presence of a Hamilton-Jacobi equation suggests a classical-mechanical interpretation. In classical mechanics the Hamiltonian (3.3) would determine the motion of a particle on Ω; $\bar\Omega \times \mathbb{R}^2$ would be interpreted as phase space, and $\boldsymbol{p} = (p_i)$, $i = 1, 2$, as the momentum of the particle. But this Hamiltonian is precisely the Wentzell-Freidlin Hamiltonian governing the large fluctuations of the process $\boldsymbol{x}_\epsilon(t)$ away from S [20]. Recall that if

$$L(x^i, \dot x^i) = \frac{1}{2} D_{ij}(\boldsymbol{x}) \left(\dot x^i - b^i(\boldsymbol{x})\right) \left(\dot x^j - b^j(\boldsymbol{x})\right) \tag{3.4}$$

is the Lagrangian canonically conjugate to $H(x^i, p_i)$, with the covariant tensor field D_{ij} defined by $D_{ij} D^{jk} = \delta_i{}^k$, then the Wentzell-Freidlin classical action function $W : \bar\Omega \to \mathbb{R}$ is defined by

$$W(\boldsymbol{x}) = \inf_{\substack{T>0 \\ \boldsymbol{q}:[0,T]\to\bar\Omega \\ \boldsymbol{q}(0)=S,\ \boldsymbol{q}(T)=\boldsymbol{x}}} \int_0^T L(\boldsymbol{q}, \dot{\boldsymbol{q}})\, dt. \tag{3.5}$$

That is, in Wentzell-Freidlin theory $W(\boldsymbol{x})$ is computed as an infimum over trajectories from S to $\boldsymbol{x}$, and is a classical action function in the sense of classical mechanics. The Wentzell-Freidlin W will necessarily satisfy the Hamilton-Jacobi equation (3.2a), so we may identify it with the function W in the outer approximation (3.1).

By the calculus of variations, if the infimum in (3.5) is achieved by a trajectory extending from S to $\boldsymbol{x}$, all portions of the trajectory that lie in Ω (rather than $\partial\Omega$) must consist of least-action (zero-energy) classical trajectories [14]. Classical trajectories $\boldsymbol{x}(\cdot)$ are the trajectories in Ω determined by H (or L); they satisfy the Euler-Lagrange equation

$$\frac{d}{dt}\left(\frac{\partial L}{\partial \dot x^i}\right) - \frac{\partial L}{\partial x^i} = 0. \tag{3.6}$$

Equivalently, if a classical trajectory is viewed as a pair of functions $(\boldsymbol{x}(\cdot), \boldsymbol{p}(\cdot))$, specifying position and momentum (*i.e.*, location in $\Omega \times \mathbb{R}^2$) as a function of time, it must satisfy Hamilton's equations. Hamilton's equations are of the form

$$\frac{d}{dt} \begin{bmatrix} x^k \\ p_k \end{bmatrix} = \begin{bmatrix} \mathbf{0} & \boldsymbol{I} \\ -\boldsymbol{I} & \mathbf{0} \end{bmatrix} \begin{bmatrix} \dfrac{\partial H}{\partial x^k} \\ \dfrac{\partial H}{\partial p_k} \end{bmatrix}, \tag{3.7}$$

and express the fact that $t \mapsto (\boldsymbol{x}(t), \boldsymbol{p}(t))$ must be an integral curve of a vector field on $\Omega \times \mathbb{R}^2$ determined by H. For the Hamiltonian (3.3) they reduce to

$$\dot x^k = \frac{\partial H}{\partial p_k} = D^{jk}(\boldsymbol{x}) p_j + b^k(\boldsymbol{x}) \tag{3.8a}$$

$$\dot p_k = -\frac{\partial H}{\partial x^k} = \partial_k D^{ij}(\boldsymbol{x}) p_i p_j + \partial_k b^i(\boldsymbol{x})\, p_i. \tag{3.8b}$$

Along the trajectory, momentum and velocity uniquely determine each other; by (3.8a),

$$p_i = D_{ij}(\boldsymbol{x})[\dot x^j - b^j(\boldsymbol{x})]. \tag{3.9}$$

Such a one-to-one correspondence is familiar from classical mechanics.

If the least-action trajectory from S to $\boldsymbol{x}$ exists and is unique, it is interpreted in Wentzell-Freidlin theory as the most probable (in the $\epsilon \to 0$ limit) fluctuational path from S to $\boldsymbol{x}$: the one whose cost is least. Since $p_i = \partial_i W$ at all points along the trajectory, $W(\boldsymbol{x})$ (the cost of the trajectory) can be computed from

$$W(\boldsymbol{x}) = \int_S^{\boldsymbol{x}} p_i \, dx^i, \tag{3.10}$$

the line integral being taken along the trajectory. Equivalently, W satisfies

$$\dot{W} = p_i \dot{x}^i = p_i[D^{ij}(\boldsymbol{x})p_j + b^i(\boldsymbol{x})], \tag{3.11}$$

an ordinary differential equation which may be integrated along the corresponding trajectory in phase space. Note however that the infimum in (3.5) will not actually be achieved at finite transit time. It is readily verified for the Hamiltonian (3.3) that zero-energy trajectories emanating from a fixed point of the drift field $\boldsymbol{b}$, such as S, will have *infinite transit time*. The formally most probable fluctuational paths require an infinite amount of time to emerge from S, and are more naturally parametrized by $t \in (-\infty, T]$. We discuss the physical consequences of this phenomenon elsewhere [34]. The integration of (3.11), as well as that of (3.8a) and (3.8b), must begin at $t = -\infty$.

For each such path $\lim_{t\to-\infty} \boldsymbol{x}(t) = S$, and by (3.9), $\lim_{t\to-\infty} \boldsymbol{p}(t) = 0$ as well. But by examination $(S, 0)$ is a fixed point (of hyperbolic type) of the deterministic flow on the phase space $\Omega \times \mathbb{R}^2$ defined by Hamilton's equations. So in the language of dynamical systems, the most probable fluctuational paths of Wentzell-Freidlin theory form the *unstable manifold* of the point $(S, 0) \in \bar{\Omega} \times \mathbb{R}^2$. This manifold, which we shall denote $\mathcal{M}^u_{(S,0)}$, is 2-dimensional; it is coordinatized (at least in a neighborhood of $(S, 0)$) by (i) the choice of outgoing trajectory, and (ii) the arc length along the trajectory. $\mathcal{M}^u_{(S,0)}$ is a *Lagrangian manifold*: it is invariant under the Hamiltonian flow. The stable manifold $\mathcal{M}^s_{(S,0)}$ of $(S, 0)$ in $\Omega \times \mathbb{R}^2$ is clearly the manifold $\boldsymbol{p} \equiv \boldsymbol{0}$, which by (3.8a) and (3.8b) is also invariant under the flow. It comprises 'cost-free' ($\Delta W = 0$) trajectories that satisfy $\dot{x}^i = b^i(\boldsymbol{x})$, and simply follow the mean drift toward S.

The analogy with Hamiltonian dynamics can be pushed much further. The action W as computed by (3.10) is a single-valued function of position on $\mathcal{M}^u_{(S,0)}$, and p_i equals $\partial_i W(\boldsymbol{x})$ at every point $(\boldsymbol{x}, \boldsymbol{p}) \in \mathcal{M}^u_{(S,0)}$. But it does not follow that W may be viewed as a single-valued function on Ω. This is because the unstable manifold may fold back on itself, and the projection $(\boldsymbol{x}, \boldsymbol{p}) \mapsto \boldsymbol{x}$ from $\mathcal{M}^u_{(S,0)}$ to $\bar{\Omega}$ may not be one-to-one. Equivalently the zero-energy classical trajectories emanating from S may cross each other, creating *caustics* [9, 17, 22, 33, 34, 35]; these caustics are the projections onto $\bar{\Omega}$ of the folds of $\mathcal{M}^u_{(S,0)}$. We shall not pursue the phenomenon of caustics at any length; unless otherwise stated we assume that the solution of the Hamilton-Jacobi equation is single-valued on $\bar{\Omega}$. In this case the map $\boldsymbol{x} \mapsto \boldsymbol{p}(\boldsymbol{x})$ will be single-valued. The projection map from $\mathcal{M}^u_{(S,0)}$ to $\bar{\Omega}$ may also fail to be onto. If this occurs, $W(\boldsymbol{x})$, for at least some $\boldsymbol{x} \in \bar{\Omega}$, cannot be viewed as the action of a classical trajectory from S to $\boldsymbol{x}$ which lies entirely in Ω; the action-minimizing trajectory, if it exists, must pass through $\partial\Omega$ on its way from S to $\boldsymbol{x}$. We shall say more about this possibility in the next section.

If we wish to compute the value of W at some point in Ω other than S, we may integrate Hamilton's equations from $(S, 0)$, continually updating $\boldsymbol{x}$ and $\boldsymbol{p}$, until the specified point is reached. The ordinary differential equation (3.11), which can be integrated simultaneously, will yield the value of W at the endpoint. But the numerical computation of K, which has no elementary classical-mechanical interpretation, is more subtle. Since $\dot{x}^i = \partial H/\partial p_i$,

$(\partial H/\partial p_i)\partial_i K$ equals $\dot{K}$, the time derivative of K along the trajectory emerging from S. So the transport equation (3.2b) becomes

$$\dot{K} = -\left[\frac{\partial^2 H}{\partial x^i \partial p_i} + \frac{1}{2}\frac{\partial^2 W}{\partial x^i \partial x^j}\frac{\partial^2 H}{\partial p_i \partial p_j}\right] K. \tag{3.12}$$

This equation cannot be integrated numerically unless the Hessian matrix $\partial_i\partial_j W$ is known at all points along the trajectory. Fortunately $\partial_i\partial_j W$ itself satisfies an ordinary differential equation, obtained as follows. Differentiating the Hamilton-Jacobi equation $H = 0$ twice with respect to position on $\mathcal{M}^u_{(S,0)}$ yields

$$\left(\frac{\partial}{\partial x^i} + \frac{\partial p_k}{\partial x_i}\frac{\partial}{\partial p_k}\right)\left(\frac{\partial}{\partial x^j} + \frac{\partial p_l}{\partial x^j}\frac{\partial}{\partial p_l}\right) H = 0. \tag{3.13}$$

By rearranging terms, and using Hamilton's equations and $\partial_i p_j = \partial_i \partial_j W$, we obtain

$$\dot{W}_{,ij} = -\frac{\partial^2 H}{\partial p_k \partial p_l} W_{,ik} W_{,jl} - \frac{\partial^2 H}{\partial x^j \partial p_k} W_{,ik} - \frac{\partial^2 H}{\partial x^i \partial p_k} W_{,jk} - \frac{\partial^2 H}{\partial x^i \partial x^j}. \tag{3.14}$$

(For notational convenience $W_{,ij}$ signifies $\partial_i\partial_j W$ henceforth; we also write ${b^i}_{,j}$ for $\partial_j b^i$, *etc*.) This inhomogeneous Riccati equation for the Hessian $W_{,ij}$ is due to the present authors [33], though Ludwig apparently used an equivalent equation in the 1970's [29]. In any event, equation (3.14) may be integrated to yield $W_{,ij}$ at all points along an outgoing Wentzell-Freidlin trajectory. In numerical work the system (3.8a), (3.8b), (3.11), (3.12), (3.14) of coupled ordinary differential equations would be integrated simultaneously to produce W and K.

At any $\boldsymbol{x} \in \Omega$, $W_{,ij}(\boldsymbol{x}) = \partial_j p_i(\boldsymbol{x})$ specifies a 2-dimensional subspace of $\mathbb{R}^4$, the tangent space $T_{(\boldsymbol{x},\boldsymbol{p}(\boldsymbol{x}))}\mathcal{M}^u_{(S,0)}$ to the unstable manifold $\mathcal{M}^u_{(S,0)} \subset \bar{\Omega} \times \mathbb{R}^2$ at $(\boldsymbol{x}, \boldsymbol{p}(\boldsymbol{x}))$. The Riccati equation (3.14) determines a trajectory through the (compact) Graßmann manifold of such 2-dimensional subspaces. This sort of interpretation is standard in the theory of matrix Riccati equations [47], and facilitates the integration of (3.14) through points where $W_{,ij}$ diverges. Such divergences occur however only when the classical trajectory encounters a caustic [17, 35]. This is because $W_{,ij}$ diverges only at points $\boldsymbol{x}$ where the tangent space $T_{(\boldsymbol{x},\boldsymbol{p}(\boldsymbol{x}))}\mathcal{M}^u_{(S,0)}$ 'turns vertical' [15]. We shall not pursue the consequences of caustics further here.

Much more could be said about the geometric interpretation of the above system of equations, which is ultimately made possible by the symplectic structure of classical mechanics on $\Omega \times \mathbb{R}^2$. We confine ourselves to pointing out the differential-geometric (coordinate-free) interpretation of the Wentzell-Freidlin fluctuational paths on Ω. The contravariant tensor field D^{ij} is naturally viewed as a Riemannian metric on Ω, and may be used to raise and lower indices. If connection coefficients (Christoffel symbols) ${\Gamma^i}_{jk}$ are defined by

$${\Gamma^i}_{jk} = \frac{1}{2} D^{il}(D_{lj,k} + D_{lk,j} - D_{kj,l}) \tag{3.15}$$

as usual, the covariant derivative ${u^i}_{;j}$ of a vector field u^i on Ω will be given by

$${u^i}_{;j} = {u^i}_{,j} + {\Gamma^i}_{jk} u^k. \tag{3.16}$$

It is easy to check that if the mean drift $\boldsymbol{b} = 0$, the Euler-Lagrange equations (3.6) for the velocity field $\dot{x}^i(\cdot)$ of the fluctuational paths on Ω reduce to the single covariant equation ${\dot{x}^i}_{;j}\dot{x}^j = 0$. This is a statement of *covariant constancy* of the velocity of each such path along itself: the most probable fluctuational paths in this case are simply the geodesics of D^{ij}

which emanate from the point S. If $\boldsymbol{b} \neq 0$ the situation is more complicated; computation yields

$$(\dot{x}^i - b^i)_{;j}\dot{x}^j + (\dot{x}^j - b^j){b_j}^{;i} = 0. \tag{3.17}$$

In a similar way, if $\boldsymbol{b} = 0$ the Riccati equation (3.14), if viewed as applying to a function W defined on Ω rather than $\mathcal{M}^u_{(S,0)}$, simplifies to yield a covariant equation related to the equations of geodesic deviation on Ω. Taking $\boldsymbol{b} \neq 0$ yields a generalization. A fuller discussion of the differential-geometric interpretation may appear elsewhere.

4. Behavior near the fixed points. The outer approximation to the principal eigenfunction v^0_ϵ of the Kolmogorov operator $\mathcal{L}^*_\epsilon$ must be supplemented by an inner approximation in a boundary region centered on the saddle point H, and an approximation in the stable region of size $\mathcal{O}(\epsilon^{1/2})$ near S. In this section we explain how our geometric picture facilitates the construction of these approximations. In particular, we shall explain why the phenomenon of skewing near H depends strongly on the parameter $\mu \stackrel{\text{def}}{=} |\lambda_s(H)|/|\lambda_u(H)|$, the ratio of the stable and unstable eigenvalues of the linearization of the drift field at H.

To a degree it is possible to construct the approximations near H and S in parallel. That is because $(H,0)$, as well as $(S,0)$, is a fixed point (of hyperbolic type) of the deterministic flow on the phase space $\bar{\Omega} \times \mathbb{R}^2$ specified by Hamilton's equations (3.8). In fact to any fixed point of the drift field $\boldsymbol{b}$ on Ω (or $\bar{\Omega}$) there corresponds a fixed point of the flow on $\Omega \times \mathbb{R}^2$ (or $\bar{\Omega} \times \mathbb{R}^2$), at zero momentum. By examination, zero-energy classical trajectories that are incident on such points in phase space, as well as those that emanate from them, will have infinite transit time. A consequence of this is that the zero-energy trajectories incident on $(H,0)$ form the stable manifold of $(H,0)$ in $\bar{\Omega} \times \mathbb{R}^2$, which we shall denote $\mathcal{M}^s_{(H,0)}$.

We are assuming that the classical action W, computed from the variational definition (3.5), attains a minimum on $\partial\Omega$ at H. We shall also assume that the infimum in the expression (3.5) for $W(H)$ is achieved; in particular, that $W(H)$ is the action of a unique zero-energy classical trajectory $\boldsymbol{q}^* : \mathbb{R} \to \Omega$ which emanates from S at time $t = -\infty$ and is incident on H at $t = \infty$. This trajectory $\boldsymbol{q}^*$, which is the formally most probable fluctuational path from S to $\partial\Omega$ as $\epsilon \to 0$, is called the *most probable exit path* (MPEP). It may be viewed as the projection of a trajectory $(\boldsymbol{q}^*, \boldsymbol{p}^*) : \mathbb{R} \to \Omega \times \mathbb{R}$ in phase space, which necessarily lies in both the unstable manifold $\mathcal{M}^u_{(S,0)}$ and the stable manifold $\mathcal{M}^s_{(H,0)}$. The intersection $\mathcal{M}^u_{(S,0)} \cap \mathcal{M}^s_{(H,0)}$ of these two 2-dimensional manifolds will consist of zero-energy trajectories from $(S,0)$ to $(H,0)$. Examples are known in which the intersection consists of more than a single trajectory [33], but generically we expect that there is a unique zero-energy trajectory from S to H with minimum action.

At all points on $\mathcal{M}^u_{(S,0)}$ the momentum p_i equals $\partial W/\partial x^i$. Since the MPEP approaches $(\boldsymbol{x},\boldsymbol{p}) = (S,0)$ as $t \to -\infty$ and $(H,0)$ as $t \to \infty$, we expect that S and H are critical points of W on $\bar{\Omega}$. To leading order, a quadratic approximation to W would seemingly be appropriate near both S and H. We shall shortly see that generically, the behavior of W near H (though not near S) is more complicated. But exploring the possible quadratic approximations to W is useful nonetheless.

The assumption of quadratic behavior near the fixed points has the following consequences. Along the MPEP, as $t \to -\infty$ or $t \to \infty$ the left-hand side of the matrix Riccati equation (3.14) will tend to zero, yielding the *algebraic* Riccati equation

$$\frac{\partial^2 H}{\partial p_k \partial p_l} W_{,ik} W_{,jl} + \frac{\partial^2 H}{\partial x^j \partial p_k} W_{,ik} + \frac{\partial^2 H}{\partial x^i \partial p_k} W_{,jk} + \frac{\partial^2 H}{\partial x^i \partial x^j} = 0 \tag{4.1}$$

for the Hessian matrix $W_{,ij} = W_{,ij}(\mathfrak{p})$ of second derivatives of W at the fixed point $\mathfrak{p}$, $\mathfrak{p} = S, H$. Here the partial derivatives of the Hamiltonian must be evaluated at $(\boldsymbol{x},\boldsymbol{p}) = (\mathfrak{p}, 0)$.

Substituting the explicit form (3.3) of the Wentzell-Freidlin Hamiltonian $H(\cdot,\cdot)$ into (4.1) yields the matrix equation

$$W_{,ij}D^{jk}W_{,kl} + W_{,ij}B^j{}_l + B^j{}_i W_{,jl} = 0 \tag{4.2}$$

for $W_{,ij}(\mathfrak{p})$. Here we have written $\boldsymbol{B} = (B^i{}_j)$ for the linearized drift field $b^i{}_{,j}(\mathfrak{p})$ at $\mathfrak{p}$, and D^{ij} signifies the diffusivity tensor $D^{ij}(\mathfrak{p})$. In matrix form, equation (4.2) reads

$$\boldsymbol{ZDZ} + \boldsymbol{ZB} + \boldsymbol{B}^t\boldsymbol{Z} = \boldsymbol{0} \tag{4.3}$$

where $\boldsymbol{Z} = \boldsymbol{Z}(\mathfrak{p}) = (W_{,ij}(\mathfrak{p})) = (\partial p_i/\partial x^j)(\mathfrak{p})$ is the 2-by-2 Hessian matrix of W at $\mathfrak{p}$. $\boldsymbol{Z}(\mathfrak{p})$ specifies a 2-dimensional subspace of $\mathbb{R}^4$, the tangent space $T_{(\mathfrak{p},0)}\mathcal{M}^u_{(S,0)}$ of the unstable manifold $\mathcal{M}^u_{(S,0)}$ at $(\mathfrak{p},0)$.

The 2-by-2 Hessian matrix $\boldsymbol{Z}(S)$ (and also the 2-by-2 Hessian matrix $\boldsymbol{Z}(H)$, if a quadratic approximation to W is valid near H) may be computed by solving the algebraic Riccati equation (4.3). The solution space of such equations as (4.3) is well understood [26]. Suffice it to say that if $\operatorname{tr}\boldsymbol{B} \neq 0$, there will be exactly four solutions: one of full rank, two of rank unity, and the trivial solution $\boldsymbol{Z} = \boldsymbol{0}$. At $\mathfrak{p} = S$ the solutions to (4.3) of less than full rank can be ruled out on physical grounds; S must be a local minimum of W, and the cost $W(\boldsymbol{x})$ of fluctuations from S to $\boldsymbol{x}$ must increase quadratically as $\boldsymbol{x} - S$ increases. Since the outer approximation to $v^0_\epsilon(\boldsymbol{x})$ is of the form $K(\boldsymbol{x})\exp(-W(\boldsymbol{x})/\epsilon)$, the matching inner approximation to v^0_ϵ near S must be a Gaussian approximation, and its inverse covariance matrix $\boldsymbol{Z}(S)$ must be of full rank [29].

We now focus on the quadratic (or putatively quadratic) behavior of W near the saddle point H. A Hessian matrix $\boldsymbol{Z}(H) = (\partial W/\partial x^i\partial x^j)(H)$, *i.e.*, $(\partial p_i/\partial x^j)(H)$, would be a *matrix of partial slopes*: It would specify the tangent space $T_{(H,0)}\mathcal{M}^u_{(S,0)}$ of the unstable manifold $\mathcal{M}^u_{(S,0)}$ at the point $(H,0)$ in phase space. Since the Lagrangian manifold $\mathcal{M}^u_{(S,0)}$ is formed from classical trajectories, the tangent space $T_{(H,0)}\mathcal{M}^u_{(S,0)}$, and hence the value of $\boldsymbol{Z}(H)$, are tightly constrained by the linearization of Hamilton's equations (3.8) at the fixed point $(H,0)$. Linearizing there yields

$$\frac{d}{dt}\begin{bmatrix}\delta\boldsymbol{x}\\ \delta\boldsymbol{p}\end{bmatrix} = \boldsymbol{T}(H)\begin{bmatrix}\delta\boldsymbol{x}\\ \delta\boldsymbol{p}\end{bmatrix}, \tag{4.4}$$

where $(\delta\boldsymbol{x},\delta\boldsymbol{p}) = (\boldsymbol{x},\boldsymbol{p}) - (H,0)$. Here the 4-by-4 matrix

$$\boldsymbol{T}(H) \stackrel{\text{def}}{=} \begin{bmatrix}\boldsymbol{B}(H) & \boldsymbol{D}(H)\\ \boldsymbol{0} & -\boldsymbol{B}(H)^t\end{bmatrix} \tag{4.5}$$

is the linearization of the Hamiltonian flow at $(H,0)$. At $(H,0)$, the manifold $\mathcal{M}^u_{(S,0)}$ must be tangent to a two-dimensional *spectral subspace* of $\boldsymbol{T}(H)$. This subspace must be the linear span (over $\mathbb{R}$) of two of the four eigenvectors of $\boldsymbol{T}(H)$.

We digress briefly to discuss the eigenvalues and eigenvectors of $\boldsymbol{T}(H)$, which have an obvious interpretation in terms of the flow of zero-energy classical trajectories in the vicinity of H. We introduce some notation: let the eigenvectors of the linearized drift $\boldsymbol{B}(H)$ with eigenvalues $\lambda_s(H) < 0$ and $\lambda_u(H) > 0$ be denoted $\boldsymbol{e}_s$ and $\boldsymbol{e}_u$. By the definition (4.5), the eigenvectors of $\boldsymbol{T}(H)$ with eigenvalues $\lambda_s(H)$ and $\lambda_u(H)$ will be $(\boldsymbol{e}_s,\boldsymbol{0})$ and $(\boldsymbol{e}_u,\boldsymbol{0})$. The eigenvectors of $\boldsymbol{T}(H)$ with eigenvalues $-\lambda_s(H)$ and $-\lambda_u(H)$ will be denoted $(\tilde{\boldsymbol{e}}_u,\tilde{\boldsymbol{g}}_u)$ and $(\tilde{\boldsymbol{e}}_s,\tilde{\boldsymbol{g}}_s)$; the interchange of subscripts is justified because $-\lambda_s(H) > 0$ and $-\lambda_u(H) < 0$, indicating instability and stability respectively. Since $(\boldsymbol{e}_s,\boldsymbol{0})$ and $(\tilde{\boldsymbol{e}}_s,\tilde{\boldsymbol{g}}_s)$ are 'contracting' eigenvectors, the tangent space $T_{(H,0)}\mathcal{M}^s_{(H,0)}$ of the stable manifold $\mathcal{M}^s_{(H,0)}$ at $(H,0)$ will be their linear span (over $\mathbb{R}$); similarly $T_{(H,0)}\mathcal{M}^u_{(H,0)}$ will be the linear span of the 'expanding' eigenvectors $(\boldsymbol{e}_u,\mathbf{0})$ and $(\tilde{\boldsymbol{e}}_u,\tilde{\boldsymbol{g}}_u)$.

We can now explain how to determine, in any generic model, which two eigenvectors of $\boldsymbol{T}(H)$ will span the tangent space of the Lagrangian manifold $\mathcal{M}^u_{(S,0)}$ at $(H,0)$. Since the MPEP $(\boldsymbol{q}^*,\boldsymbol{p}^*):\mathbb{R}\to\mathcal{M}^u_{(S,0)}\subset\Omega\times\mathbb{R}$ is incident on $(H,0)$ as $t\to\infty$, and is a classical trajectory, we have the asymptotic approximation

$$(\boldsymbol{q}^*(t),\boldsymbol{p}^*(t))\sim(H,0)+a_s e^{-|\lambda_s(H)|t}(\boldsymbol{e}_s,\mathbf{0})+\tilde{a}_s e^{-\lambda_u(H)t}(\tilde{\boldsymbol{e}}_s,\tilde{\boldsymbol{g}}_s) \tag{4.6}$$

as $t\to\infty$. Only the two stable eigenvectors enter; the coefficients a_s and $\tilde{a}_s$ are model-dependent, and generically are both nonzero. The tangent space $T_{(H,0)}\mathcal{M}^u_{(S,0)}$ is formed by zero-energy classical trajectories emanating from $(S,0)$ that are perturbations of the MPEP. To leading order, each such perturbed trajectory must be of the form

$$\begin{aligned}(\boldsymbol{q}^*(t),\boldsymbol{p}^*(t))+\alpha\Big[&b_s e^{-|\lambda_s(H)|t}(\boldsymbol{e}_s,\mathbf{0})+\tilde{b}_s e^{-\lambda_u(H)t}(\tilde{\boldsymbol{e}}_s,\tilde{\boldsymbol{g}}_s)\\ &+b_u e^{\lambda_u(H)t}(\boldsymbol{e}_u,\mathbf{0})+\tilde{b}_u e^{|\lambda_s|(H)t}(\tilde{\boldsymbol{e}}_u,\tilde{\boldsymbol{g}}_u)\Big],\end{aligned} \tag{4.7}$$

where α is a parameter that indexes the trajectories. The coefficients b_s, $\tilde{b}_s$, b_u, $\tilde{b}_u$ are also model-dependent and generically nonzero.

Generically, the MPEP $\boldsymbol{q}^*$ will approach $(H,0)$ as $t\to\infty$ along the *less* contractive direction in phase space; the stochastic model would have to be carefully 'tuned' for the incoming MPEP to approach along the *more* contractive direction in (4.6). If $\mu<1$, $-\lambda_u(H)<\lambda_s(H)<0$ and $\lambda_s(H)$ is less contractive; in this case the MPEP will generically approach H as $\exp(-|\lambda_s(H)|t)$. Similarly if $\mu>1$, $\lambda_s(H)<-\lambda_u(H)<0$ and the MPEP will generically approach H as $\exp(-\lambda_u(H)t)$. Since $\partial_i b^i(H)=\lambda_s(H)+\lambda_u(H)$, this implies that in phase space the MPEP will generically approach the fixed point $(H,0)$ along the tangent vector $(\boldsymbol{e}_s,\mathbf{0})$ if $\partial_i b^i(H)>0$, and along $(\tilde{\boldsymbol{e}}_s,\tilde{\boldsymbol{g}}_s)$ if $\partial_i b^i(H)<0$.

A similar analysis, applied to (4.7), shows that the tangent space to the manifold $\mathcal{M}^u_{(S,0)}$ at $(H,0)$ must include, besides the contracting eigenvector $(\boldsymbol{e}_s,\mathbf{0})$ or $(\tilde{\boldsymbol{e}}_s,\tilde{\boldsymbol{g}}_s)$, the *more* expansive of the two expanding eigenvectors. When $\mu<1$, the more expansive eigenvector is $(\boldsymbol{e}_u,\mathbf{0})$; when $\mu>1$, it is $(\tilde{\boldsymbol{e}}_u,\tilde{\boldsymbol{g}}_u)$. We conclude that the tangent space $T_{(H,0)}\mathcal{M}^u_{(S,0)}$ is generically equal to the subspace $\mathrm{sp}\{(\boldsymbol{e}_s,\mathbf{0}),(\boldsymbol{e}_u,\mathbf{0})\}$ when $\mu<1$, and to the subspace $\mathrm{sp}\{(\tilde{\boldsymbol{e}}_s,\tilde{\boldsymbol{g}}_s),(\tilde{\boldsymbol{e}}_u,\tilde{\boldsymbol{g}}_u)\}$ when $\mu>1$. It is easy to see that the former alternative corresponds to the Hessian matrix $\boldsymbol{Z}(H)$ equalling $\mathbf{0}$, and the latter alternative to the Hessian matrix being of full rank.

We can now resolve the question of the extent to which the behavior of W near H can be genuinely quadratic. Much light is thrown on this question by a sketch of the pattern of zero-energy classical trajectories emanating from S, when prolonged to the vicinity of H. These trajectories, which include the MPEP $(\boldsymbol{q}^*,\boldsymbol{p}^*)$, lie in the manifold $\mathcal{M}^u_{(S,0)}$. If projected 'down' from $\mathcal{M}^u_{(S,0)}$ to Ω by the map $(\boldsymbol{x},\boldsymbol{p})\mapsto\boldsymbol{x}$, it follows from the preceding analysis that they will generically trace out in the immediate vicinity of H the hyperbolic patterns shown in Figs. 4.1(a) and 4.1(b). The principal axes of the hyperbolæ are $\boldsymbol{e}_s$ and $\boldsymbol{e}_u$ if $\mu<1$, and $\tilde{\boldsymbol{e}}_s$ and $\tilde{\boldsymbol{e}}_u$ if $\mu>1$. By convention, we assume that the $\boldsymbol{e}_s$ ray is vertical, that Ω is to the right of the $\boldsymbol{e}_s$ ray, and that the MPEP approaches H from the first quadrant.

Figure 2(a) reveals an unusual phenomenon: Since the stable eigenvector $\boldsymbol{e}_s$ of $\boldsymbol{B}(H)$ lies in $\partial\Omega$, the MPEP $\boldsymbol{q}^*$ will generically be tangent to the boundary $\partial\Omega$ in stochastic models with $\mu<1$. This 'grazing MPEP' effect has been seen in numerical studies [53]. Also, since the $\mu<1$ solution for $\boldsymbol{Z}(H)$ is the 2-by-2 zero matrix, when $\mu<1$ we necessarily have

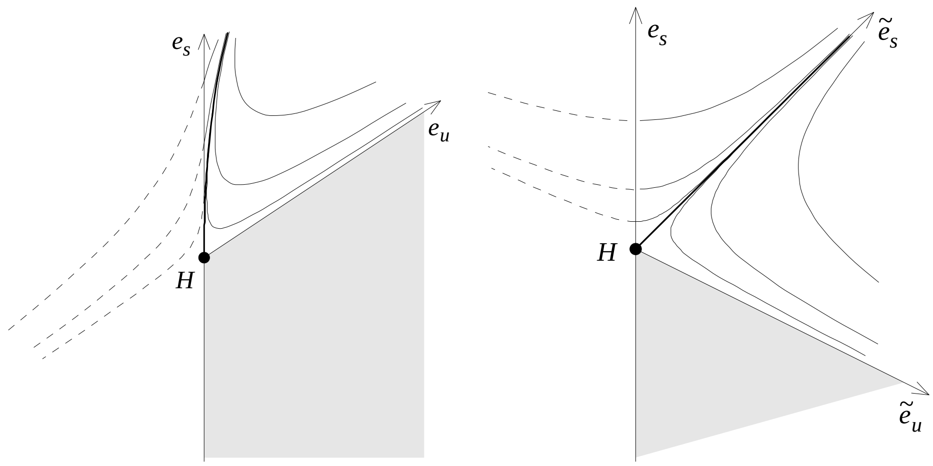

FIG. 4.1. *The generic appearance of the flow near H of the zero-energy classical trajectories emanating from S; equivalently, the Hamiltonian flow on the manifold $\mathcal{M}^u_{(S,0)}$ projected 'down' to configuration space by the map $(\boldsymbol{x},\boldsymbol{p}) \mapsto \boldsymbol{x}$. Part (a) of the figure illustrates the case $\mu < 1$,* i.e., *$\partial_i b^i(H) > 0$; part (b), the case $\mu > 1$,* i.e., *$\partial_i b^i(H) < 0$. In both cases the MPEP [most probable exit path] is the solid curve incident on H. The wedge-shaped shaded regions are classically forbidden; also, the dashed trajectories (which extend beyond the $\boldsymbol{e}_s$ ray, which lies in $\partial\Omega$) are unphysical.*

that $W_{,ij}(\boldsymbol{x}) \to 0$ as $\boldsymbol{x} \to H$ along the MPEP. This 'flat' behavior of W near H has an appealing physical explanation: As $t \to \infty$ the most probable exit paths (perturbations of the grazing MPEP) come close to following the drift field $\boldsymbol{b}$ (they "fall in"). Thus very little additional action (cost) is built up as H is approached, in models with $\mu < 1$. This effect too has been seen in numerical studies [6, 53].

We have not commented yet on the most visible feature of Figs. 4.1(a) and 4.1(b), which is highly disconcerting: for both $\mu < 1$ and $\mu > 1$ there is a wedge-shaped region near H, beyond the boundary ray $\boldsymbol{e}_u$ and the boundary ray $\tilde{\boldsymbol{e}}_u$ respectively, which is not reached by any of the most probable fluctuational paths. This wedge, the generic presence of which has been confirmed numerically, is 'classically forbidden' in that it cannot be reached by any zero-energy classical trajectory emanating from S. Unless the boundary ray lies in $\partial\Omega$, the wedge has nonempty interior. The presence of an unreachable region has a very simple interpretation: *Generically, the projection map $(\boldsymbol{x},\boldsymbol{p}) \mapsto \boldsymbol{x}$ from the Lagrangian manifold $\mathcal{M}^u_{(S,0)}$ to $\bar{\Omega}$ is not onto: its range does not include all of Ω.* The possibility that the projection map might fail to be onto on account of folds in the manifold $\mathcal{M}^u_{(S,0)}$ was mentioned in Section 3, but that this failure is generic is a new result.

We expect that $W(\boldsymbol{x})$, for any $\boldsymbol{x}$ in the wedge, is the action of an action-minimizing trajectory which passes through $\partial\Omega$ on its way from S to $\boldsymbol{x}$. (Cf. Day and Darden [14].) Only the portions of the trajectory that lie in Ω (rather than $\partial\Omega$) will be classical, *i.e.*, will be solutions of the Euler-Lagrange equation. The trajectory will be *piecewise classical*: it will have at least one 'corner,' or bend. The fact that generically, such fluctuational paths need to be considered for at least some endpoints $\boldsymbol{x}$ in any neighborhood of H has not been fully realized.

By a careful optimization over piecewise classical trajectories it is possible to work out, for $\boldsymbol{x}$ in the wedge, the leading dependence of $W(\boldsymbol{x})$ on $\delta\boldsymbol{x} = \boldsymbol{x} - H$ in the vicinity of H. But we may economize on effort by applying our previous results. Suppose for the sake of argument that to leading order $W(\boldsymbol{x})$ in the wedge behaves quadratically as $\boldsymbol{x} \to H$. Then the quadratic dependence will be specified by a limiting Hessian matrix $\widehat{\boldsymbol{Z}}(H) = (\widehat{W}_{,ij}(H))$, which must satisfy the algebraic Riccati equation (4.3). Moreover, $W(\boldsymbol{x})$ at any point in the wedge must be the classical action of a zero-energy trajectory extending from H to $\boldsymbol{x}$. Near H each such phase-space trajectory, when parametrized by $t > -\infty$, should be of the form

$$t \mapsto (H, 0) + C_u e^{\lambda_u(H)t}(\boldsymbol{e}_u, \boldsymbol{0}) + \tilde{C}_u e^{|\lambda_s(H)|t}(\tilde{\boldsymbol{e}}_u, \tilde{\boldsymbol{g}}_u), \tag{4.8}$$

for C_u, $\tilde{C}_u$ two constants that determine the trajectory. This is because $(\boldsymbol{e}_u, \boldsymbol{0})$ and $(\tilde{\boldsymbol{e}}_u, \tilde{\boldsymbol{g}}_u)$ are the two expanding eigenvectors of the linearization $\boldsymbol{T}(H)$. At $(H, 0)$, the Lagrangian manifold formed by these outgoing trajectories will be tangent to the subspace sp $\{(\boldsymbol{e}_u, \boldsymbol{0}), (\tilde{\boldsymbol{e}}_u, \tilde{\boldsymbol{g}}_u)\}$, and the corresponding 2-by-2 Hessian matrix $\boldsymbol{Z}(H)$ will have rank 1. In general each such trajectory will be tangent (as $t \to -\infty$, or as the trajectories emerge from H) to whichever is the *less* expansive of the two eigenvectors of $\boldsymbol{T}(H)$. If $\mu < 1$ this is $(\tilde{\boldsymbol{e}}_u, \tilde{\boldsymbol{g}}_u)$; if $\mu > 1$ it is $(\boldsymbol{e}_u, \boldsymbol{0})$.

Figure 4.2 is an extended version of Fig. 4.1, which includes the rays $\tilde{\boldsymbol{e}}_u$ and $\boldsymbol{e}_u$, and the additional trajectories (emanating from H, and tangent to them) predicted by the assumption of quadratic behavior of W in the wedge. The $\mu < 1$ case has two subcases, shown in Figs. 4.2(a) and 4.2(b). We shall refer to them as Subcase A and Subcase B; they differ in only one essential way: in the *relative* placement of the rays $\tilde{\boldsymbol{e}}_u$ and $\boldsymbol{e}_u$. We shall show in the next section that when $\mu > 1$, the $\boldsymbol{e}_u$ ray necessarily lies between the $\tilde{\boldsymbol{e}}_s$ and $\tilde{\boldsymbol{e}}_u$ rays. This situation is shown in Fig. 4.2(c); when $\mu > 1$, there are no subcases.

Subcase A of the case $\mu < 1$ is the most straightforward. It is clear from a glance at Fig. 4.2(a) that in this subcase, the action-minimizing trajectory from S to any point in the wedge is a prolongation of the MPEP: it extends from S to H, experiences a discontinuous change in direction, and then enters the wedge. Interestingly, points on $\partial\Omega$ that are on the 'wedge side' of H are reached only *viâ* trajectories that make a second passage through Ω.

We stress that these 'bent' trajectories have a physical interpretation. By Wentzell-Freidlin theory, any point $\boldsymbol{x}$ in the interior of the wedge is (as $\epsilon \to 0$) preferentially reached during large fluctuations away from S by a bent trajectory. That is, when $\mu < 1$ the fluctuation will in Subcase A preferentially drive the random process $\boldsymbol{x}_\epsilon(t)$ to the vicinity of H *via* the MPEP $\boldsymbol{q}^*$, before the wedge is traversed and the vicinity of $\boldsymbol{x}$ is finally reached. Although Fig. 4.2(a) displays only the portion of the wedge in the vicinity of H (*i.e.*, the wedge as computed in the linear approximation), studies of particular models show that it may extend a considerable distance from H. The numerical computation of $W(\boldsymbol{x})$, for $\boldsymbol{x}$ in the wedge, requires an integration along the appropriate bent trajectory terminating at $\boldsymbol{x}$.

There is a problem extending these conclusions to Subcase B, and to the case $\mu > 1$. It is clear from Figs. 4.2(b) and (c) that classical trajectories emanating from H which are of the form

$$t \mapsto H + C_u e^{\lambda_u(H)t}\boldsymbol{e}_u + \tilde{C}_u e^{|\lambda_s(H)|t}\tilde{\boldsymbol{e}}_u, \tag{4.9}$$

and which are tangent to the $\tilde{\boldsymbol{e}}_u$ ray (resp. the $\boldsymbol{e}_u$ ray), are necessarily *unphysical*. They are the dashed trajectories that penetrate into the complement of $\bar{\Omega}$ before returning to $\partial\Omega$ and passing through the wedge. This is quite different from Subcase A, where the trajectories emanating from H penetrate immediately into the wedge. Since the putative Hessian matrix $\widehat{\boldsymbol{Z}}(H)$ corresponds to an unphysical (impossible) velocity field $\dot{\boldsymbol{x}}(\cdot)$ for the most probable fluctuational paths, in Subcase B and when $\mu < 1$ the action in the wedge will *not* behave quadratically near H. In Subcase B and when $\mu < 1$, the flow field of the action-minimizing trajectories within the wedge will differ from the predictions of the quadratic approximation, as displayed in Figs. 4.2(b) and 4.2(c). Nonetheless, in these two cases the true action-

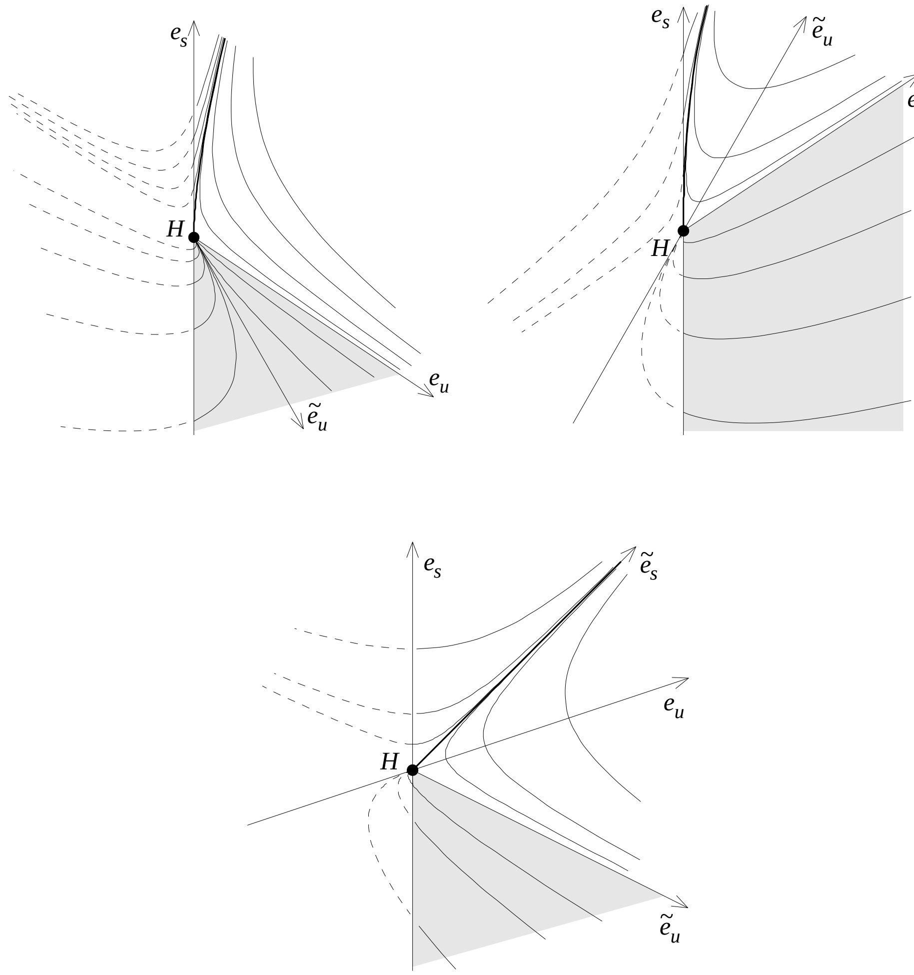

FIG. 4.2. *The generic appearance of the flow near H of the most probable fluctuational paths (*i.e.*, the action-minimizing trajectories) emanating from S. The $\boldsymbol{e}_s$ ray lies in $\partial\Omega$. Parts (a) and (b) of the figure illustrate Subcases A and B of the case $\mu < 1$; they differ in the relative placement of the $\tilde{\boldsymbol{e}}_u$ and $\boldsymbol{e}_u$ rays. Part (c) illustrates the case $\mu > 1$. In all three parts the MPEP [most probable exit path] is the solid curve incident on H. The other trajectories include zero-energy classical trajectories of the sort shown in Fig. 4.1, and 'bent' trajectories which are prolongations (piecewise classical rather than classical) of the MPEP. The classically forbidden wedge-shaped shaded regions are reached (as $\epsilon \to 0$) only* via *bent trajectories. The hyperbolic shape of the bent trajectories is strictly correct only if the classical action W behaves quadratically in the wedge-shaped regions.*

minimizing trajectory from H to any point $\boldsymbol{x}$ in the wedge should extend along $\partial\Omega$ before reentering the wedge.

We summarize our geometric interpretation in Table 4.1. The behavior of W near H, both inside and outside the wedge and for both $\mu < 1$ and $\mu > 1$, is quadratic and fully understood with the exception of the behavior inside the wedge in Subcase B, and when $\mu > 1$. Even these difficult cases lend themselves to a partial analysis. The precise behavior of W inside the wedge in Subcase B and when $\mu > 1$, even in the linear approximation near H, can only be obtained by solving a difficult variational problem. But it is clear on physical grounds that $W(\boldsymbol{x})$ approaches $W(H)$ quadratically as $\boldsymbol{x}$ approaches H along $\partial\Omega$ from the wedge side of H. That is because on the wedge side of H, the cost function $W(\boldsymbol{x})$ on $\partial\Omega$

TABLE 4.1

The generic limiting behavior (as $\boldsymbol{x} \to H$) of the Hessian matrix $\boldsymbol{Z}(\boldsymbol{x}) = (W_{,ij}(\boldsymbol{x}))$, and of the corresponding tangent space $T_{(\boldsymbol{x},\boldsymbol{p}(\boldsymbol{x}))}\mathcal{M}^u_{(S,0)} \subset \mathbb{R}^4$. $\boldsymbol{Z}(\boldsymbol{x}) \to \boldsymbol{Z}(H)$ if $\boldsymbol{x} \to H$ from outside the wedge, i.e., *along the manifold $\mathcal{M}^u_{(S,0)}$. Similarly $T_{(\boldsymbol{x},\boldsymbol{p}(\boldsymbol{x}))}\mathcal{M}^u_{(S,0)} \to \mathcal{N}(H)$. In Subcase A of the case $\mu < 1$, $\boldsymbol{Z}(\boldsymbol{x}) \to \widehat{\boldsymbol{Z}}(H)$ as $\boldsymbol{x} \to H$ from within the wedge; similarly $T_{(\boldsymbol{x},\boldsymbol{p}(\boldsymbol{x}))}\mathcal{M}^u_{(S,0)} \to \widehat{\mathcal{N}}(H)$. Each of $\mathcal{N}(\mathcal{H})$ and $\widehat{\mathcal{N}}(H)$, if defined, is the linear span of a pair of eigenvectors of the linearized Hamiltonian flow $\boldsymbol{T}(H)$. In Subcase B and when $\mu > 1$, the behavior of the action in the wedge is not quadratic near H, and no limiting Hessian matrix exists.*

Case [Subcase]	$\boldsymbol{Z}(H)$	$\widehat{\boldsymbol{Z}}(H)$	$\mathcal{N}(H)$	$\widehat{\mathcal{N}}(H)$
$\mu < 1$, *i.e.*, $\partial_i b^i(H) > 0$ [A]	$\mathbf{0}$	rank-1	$\mathrm{sp}\{(\boldsymbol{e}_s, 0), (\boldsymbol{e}_u, 0)\}$	$\mathrm{sp}\{(\boldsymbol{e}_u, 0), (\tilde{\boldsymbol{e}}_u, \tilde{\boldsymbol{g}}_u)\}$
$\mu < 1$, *i.e.*, $\partial_i b^i(H) > 0$ [B]	$\mathbf{0}$	—	$\mathrm{sp}\{(\boldsymbol{e}_s, 0), (\boldsymbol{e}_u, 0)\}$	—
$\mu > 1$, *i.e.*, $\partial_i b^i(H) < 0$	rank-2	—	$\mathrm{sp}\{(\tilde{\boldsymbol{e}}_s, \tilde{\boldsymbol{g}}_s), (\tilde{\boldsymbol{e}}_u, \tilde{\boldsymbol{g}}_u)\}$	—

satisfies (in Subcase B, and when $\mu > 1$)

$$W(\boldsymbol{x}) - W(H) = \int_H^{\boldsymbol{x}} p_i \, dx^i, \tag{4.10}$$

the line integral being taken along $\partial\Omega$ from H to $\boldsymbol{x}$. Here the momentum $\boldsymbol{p} = \boldsymbol{p}(\boldsymbol{x})$, at any point $\boldsymbol{x} \in \partial\Omega$, takes a value determined by (i) the zero-energy constraint, and (ii) the constraint that the corresponding velocity $\dot{\boldsymbol{x}}$ lie in $\partial\Omega$.

In Subcase A, in general $\boldsymbol{Z}(H) \neq \widehat{\boldsymbol{Z}}(H)$. In Subcase B and when $\mu > 1$ there is no reason why the quadratic growth of W along $\partial\Omega$, on the wedge side of H, should equal the quadratic growth on the other side (which arises from $\boldsymbol{Z}(H)$, rather than from (4.10)). So generically, *W will fail to be twice continuously differentiable at H.* This conclusion justifies the statements about the one-sided derivatives $\partial^2 W/\partial s^2(s = 0\pm)$ made in the Introduction. Generically these two quantities will be different; in fact if $\mu < 1$, the second derivative on the wedge side, as displayed in Table 4.1, will equal zero. We see that the difference between the two sides of the saddle point is the underlying cause of the skewing phenomenon. We also see that skewing in models with $\mu < 1$ and $\mu > 1$ will be radically different.

It bears noting that the classical action W will generically fail to be a twice continuously differentiable function of $\boldsymbol{x}$ not merely at $\boldsymbol{x} = H$, but along the entire boundary of the wedge. This is reminiscent of the Stokes phenomenon, which occurs in the asymptotic expansion of the solution (in the complex plane) of an ordinary differential equation with a small parameter multiplying the term with highest derivative. The exponent of the dominant exponential factor in the expansion is non-smooth along certain curves (anti-Stokes lines) emanating from turning points. It is probably best to view the phenomenon of the wedge as a two-dimensional version of the Stokes phenomenon. For the forward Kolmogorov equation on $\Omega \subset \mathbb{R}^2$, which is a *partial* differential equation, the anti-Stokes line appears as a curve in Ω (the boundary of the wedge) rather than in the complex plane. To see it, no analytic continuation is required.

5. Generic and non-generic inner approximations. In the following three sections our treatment becomes more quantitative. We shall approximate the principal eigenfunction v_ϵ^0 and the process $\boldsymbol{x}_\epsilon(t)$ in the boundary region near H, and study the implications for the small-ϵ asymptotics of the exit location density. In this section, we focus on the Gaussian far-field behavior of the inner approximation, and the Gaussian tails of the exit location distribution. We rederive the classical ('Eyring') formula for the small-ϵ MFPT asymptotics, and determine for the first time the limits of its validity.

If an inner approximation to v_ϵ^0, valid in the boundary region near H, is to match to the outer approximation $K(\boldsymbol{x})\exp\left(-W(\boldsymbol{x})/\epsilon\right)$, it must in the far field have leading asymptotics

$$v_\epsilon^0(\boldsymbol{x}) \sim \text{const} \times \exp\left[-(x^i - H^i)W_{,ij}(H)(x^j - H^j)/2\epsilon\right]. \tag{5.1}$$

But this statement must be interpreted with care. By convention $W_{,ij}(H)$ signifies the limiting Hessian matrix obtained by taking $\boldsymbol{x} \to H$ along the most probable exit path (MPEP), or in general from within the complement of the classically forbidden 'wedge.' So the statement (5.1) holds when $(\boldsymbol{x} - H)/\epsilon^{1/2} \to \infty$ within the complement of the wedge. If the behavior of W in the wedge is quadratic near H, the limiting Hessian matrix obtained by taking $\boldsymbol{x} \to H$ from within the wedge is denoted $\widehat{W}_{,ij}(H)$. We saw in the last section that in Subcase A of the case $\partial_i b^i(H) > 0$ (*i.e.*, when $\mu < 1$), the behavior of W in the wedge is indeed quadratic near H, so the counterpart to (5.1) (involving $\widehat{W}_{,ij}(H)$) should hold as $(\boldsymbol{x} - H)/\epsilon^{1/2} \to \infty$ within the wedge. In other words the far-field asymptotics of the inner approximation to v_ϵ^0 must in this case be *piecewise bivariate Gaussian*: different decay (or growth) rates will be found in the wedge and its complement. In Subcase B or when $\partial_i b^i(H) < 0$ (*i.e.*, $\mu > 1$), the behavior of W in the wedge will not be quadratic near H. But even so, the inner approximation to v_ϵ^0 must still have Gaussian asymptotics as $(\boldsymbol{x} - H)/\epsilon^{1/2} \to \infty$ along the boundary $\partial\Omega$, with different decay rates on the two sides of H.

The inner approximation to v_ϵ^0 can be constructed, at least in principle, by solving a linearized version of the (approximate) forward Kolmogorov equation $\mathcal{L}_\epsilon^*\rho = 0$ in the boundary region near H. In the linear approximation we take $b^i(\boldsymbol{x}) \approx B^i{}_j(H)(x^j - H^j)$ and $D^{ij}(\boldsymbol{x}) \approx D^{ij}(H)$, so the Kolmogorov equation reduces to

$$(\epsilon/2)D^{ij}(H)\partial_i\partial_j\rho - \partial_i[B^i{}_j(H)(x^j - H^j)\rho] = 0. \tag{5.2}$$

Assume for the moment that the appropriate lengthscale on which the inner approximation should be defined is the $\mathcal{O}(\epsilon^{1/2})$ lengthscale. If so, we can employ the 'stretched' variable $X^i = (x^i - H^i)/\epsilon^{1/2}$, in terms of which (5.2) becomes

$$\frac{1}{2}D^{ij}(H)\frac{\partial^2\rho}{\partial X^i\partial X^j} - B^i{}_j(H)\frac{\partial}{\partial X^i}[X^j\rho] = 0. \tag{5.3}$$

We can change variables to reduce this covariant equation to a noncovariant, but more understandable form. Under a linear change of variables $(X')^i = L^i{}_jX^j$, *i.e.*, $\boldsymbol{X}' = \boldsymbol{L}\boldsymbol{X}$, the matrices $\boldsymbol{B}(H)$ and $\boldsymbol{D}(H)$ transform to $\boldsymbol{L}\boldsymbol{B}(H)\boldsymbol{L}^{-1}$ and $\boldsymbol{L}\boldsymbol{D}(H)\boldsymbol{L}$ respectively. Choosing $\boldsymbol{L} = \boldsymbol{D}(H)^{-1/2}$ transforms $\boldsymbol{D}(H)$ to the identity matrix. But since H is a saddle point, irrespective of coordinate transformations the linearized drift $\boldsymbol{B}(H)$ will have one positive eigenvalue ($\lambda_s(H)$) and one negative eigenvalue ($\lambda_u(H)$). By a further change of variables (a rotation) we can set $B^1{}_2(H) = 0$. So we can choose

$$\boldsymbol{B}(H) = \begin{bmatrix} \lambda_u(H) & 0 \\ c & \lambda_s(H) \end{bmatrix}, \tag{5.4}$$

for some real constant c. The constant c is not determined by $\lambda_u(H)$ and $\lambda_s(H)$. Since $\boldsymbol{D}(H) = \boldsymbol{I}$ is preserved under rotations, with respect to the new system of coordinates equation (5.3) becomes

$$\begin{aligned} &\frac{1}{2}\frac{\partial^2\rho}{\partial(X^1)^2} + \frac{1}{2}\frac{\partial^2\rho}{\partial(X^2)^2} \\ &- \lambda_u(H)\frac{\partial}{\partial X^1}[X^1\rho] - \lambda_s(H)\frac{\partial}{\partial X^2}[X^2\rho] - c\frac{\partial}{\partial X^2}[X^1\rho] = 0. \end{aligned} \tag{5.5}$$

In terms of the transformed coordinates (X^1, X^2) we may take the region Ω to be the right-half plane $X^1 > 0$, and its boundary $\partial\Omega$ to be the X^2-axis. This was the convention of Figs. 4.1 and 4.2.

This system of coordinates is computationally easy to work with. Suppose for simplicity that $\lambda_u(H) = 1$; this is an innocuous normalization condition that can be absorbed into a redefinition of time t (and noise strength ϵ). Then

$$\boldsymbol{B}(H) = \begin{bmatrix} 1 & 0 \\ c & -\mu \end{bmatrix}, \tag{5.6}$$

where $\mu \stackrel{\text{def}}{=} |\lambda_s(H)|/\lambda_u(H)$, as usual. The Kolmogorov equation (5.5) reduces to

$$\frac{1}{2}\frac{\partial^2 \rho}{\partial (X^1)^2} + \frac{1}{2}\frac{\partial^2 \rho}{\partial (X^2)^2} - \frac{\partial}{\partial X^1}[X^1\rho] + \mu\frac{\partial}{\partial X^2}[X^2\rho] - c\frac{\partial}{\partial X^2}[X^1\rho] = 0. \tag{5.7}$$

Also, a bit of matrix computation, using the form (5.6) for $\boldsymbol{B}(H)$ and $\boldsymbol{D}(H) = \boldsymbol{I}$, yields

$$(\boldsymbol{e}_s, 0) = (0, 1, 0, 0) \tag{5.8a}$$

$$(\boldsymbol{e}_u, 0) = (\mu + 1, c, 0, 0) \tag{5.8b}$$

$$(\tilde{\boldsymbol{e}}_s, \tilde{\boldsymbol{g}}_s) = (\mu - 1, c, -2\mu + 2, 0) \tag{5.8c}$$

$$(\tilde{\boldsymbol{e}}_u, \tilde{\boldsymbol{g}}_u) = (-2\mu c, \mu^2 - 1 - c^2, -2\mu c(\mu - 1), 2\mu(\mu^2 - 1)) \tag{5.8d}$$

for the four eigenvectors of the linearized Hamiltonian flow $\boldsymbol{T}(H)$ at the point $(H, 0)$ in phase space, as given by (4.5). (Normalization is irrelevant here; the negatives of these vectors could equally well have been chosen.) That $\boldsymbol{e}_s = (0, 1)$ agrees with the convention of Figs. 4.1 and 4.2.

We note in passing that the formulæ (5.8) explain the positioning of the rays $\boldsymbol{e}_u$, $\tilde{\boldsymbol{e}}_s$, and $\tilde{\boldsymbol{e}}_u$ in Figs. 4.2(a), 4.2(b), and 4.2(c). Recall that in those figures the MPEP was taken to approach from the first quadrant; if $\mu < 1$, it is generically tangent to $\boldsymbol{e}_s$, and hence to the positive X^2-axis. By examination of (5.8), if $\mu < 1$ and $c < 0$ then $\boldsymbol{e}_u$ will lie between the positive X^2-axis and $\tilde{\boldsymbol{e}}_u$, while if $c > 0$ then $\tilde{\boldsymbol{e}}_u$ (taken to point into the right half-plane) will lie between the positive X^2-axis and $\boldsymbol{e}_u$. So the Subcases A and B of Figs. 4.2(a) and 4.2(b) are simply the subcases $c < 0$ and $c > 0$. This correspondence assumes of course that the MPEP is tangent to the *positive* X^2-axis; if it approached H from the fourth quadrant, and were tangent to the negative X^2-axis instead, then the interpretation in terms of $\operatorname{sgn} c$ would be reversed.

Formulæ (5.8) justify the positioning of the rays in Fig. 4.2(c), as well. If $\mu > 1$, we know by the arguments of the last section that the approaching MPEP is generically tangent to $\tilde{\boldsymbol{e}}_s$. By (5.8c), $\tilde{\boldsymbol{e}}_s \propto (\mu - 1, c)$, and our convention that the MPEP approaches from the first quadrant mandates that $c \geq 0$. It is easy to verify, by examining (5.8), that in the right-half plane, when $\mu > 1$ and $c > 0$ the $\boldsymbol{e}_u$ ray necessarily lies between the the $\tilde{\boldsymbol{e}}_s$ ray and the the $\tilde{\boldsymbol{e}}_u$ ray. This was the positioning of Fig. 4.2(c).

In our new coordinate system, it is easy to study quantitatively the quadratic behavior of the action W near the saddle point. Substituting (5.6) into the Riccati equation (4.3), and solving, gives

$$\boldsymbol{Z}(H) = \frac{2(\mu - 1)}{(\mu - 1)^2 + c^2}\begin{bmatrix} c^2 + 1 - \mu & -c\mu \\ -c\mu & \mu^2 - \mu \end{bmatrix} \tag{5.9}$$

as the formula for the rank-2 Hessian matrix $\boldsymbol{Z}(H) = [W_{,ij}(H)] = [\partial p_i/\partial x^j(H)]$. Recall that generically this limiting Hessian matrix arises (when $\boldsymbol{x} \to H$ in the complement of the wedge) only when $\mu > 1$. If $\mu < 1$, $\boldsymbol{Z}(\boldsymbol{x}) \to \boldsymbol{0}$ as $\boldsymbol{x} \to H$ along the MPEP.

The quadratic behavior of W in the wedge (to the extent that it *is* quadratic) can be computed similarly. In Subcase A of $\mu < 1$, the limiting Hessian matrix $\widehat{\boldsymbol{Z}}(H)$ in the wedge exists, and equals by Table 4.1 the rank-1 matrix corresponding to the tangent space sp $\{(\boldsymbol{e}_u, 0), (\tilde{\boldsymbol{e}}_u, \tilde{\boldsymbol{g}}_u)\}$. The formula

$$\widehat{\boldsymbol{Z}}(H) = \frac{2\mu}{c^2 + (\mu+1)^2} \begin{bmatrix} c^2 & -c(\mu+1) \\ -c(\mu+1) & (\mu+1)^2 \end{bmatrix} \tag{5.10}$$

follows from (5.8) by some elementary manipulations. In Subcase B, and when $\mu > 1$, the behavior of $W(\boldsymbol{x})$ in the wedge as $\boldsymbol{x} \to H$ will not be quadratic. However, it follows from the formula (4.10) that its behavior as $\boldsymbol{x} \to H$ along $\partial\Omega$ (from the wedge side) *is* quadratic, with limiting second derivative

$$\widehat{Z}_{\partial\Omega}(H) = 2\mu. \tag{5.11}$$

This limiting second derivative has a simple interpretation: on the wedge side of H, the cost (action) of the most probable trajectory leading to any point on $\partial\Omega$ arises from the drift $\boldsymbol{b}$ on $\partial\Omega$ itself. (By (5.6), the drift along $\partial\Omega$ is proportional to μ.)

The formulæ (5.9)–(5.11) make quite precise the far-field ($\boldsymbol{X} \to \infty$) Gaussian (or inverted Gaussian) asymptotics that must be imposed on the solution $\rho(X^1, X^2)$ of the transformed Kolmogorov equation (5.7). First, to leading order we must have

$$\rho(X^1, X^2) \sim \exp\left(-\boldsymbol{X}^t \boldsymbol{Z}(H) \boldsymbol{X}/2\right), \qquad \boldsymbol{X} \to \infty \text{ outside the wedge.} \tag{5.12}$$

Also, in Subcase A of $\mu < 1$ we must have

$$\rho(X^1, X^2) \sim \exp\left(-\boldsymbol{X}^t \widehat{\boldsymbol{Z}}(H) \boldsymbol{X}/2\right), \qquad \boldsymbol{X} \to \infty \text{ inside the wedge.} \tag{5.13}$$

In Subcase B of $\mu < 1$, or when $\mu > 1$, we must have

$$\rho(X^1, X^2) \sim \exp\left(-\widehat{Z}_{\partial\Omega}(H)\, (X^2)^2/2\right), \qquad \boldsymbol{X} \to \infty \text{ along } \partial\Omega\text{, on the wedge side,} \tag{5.14}$$

since the boundary $\partial\Omega$ is the X^2-axis. The Dirichlet boundary condition $\rho(0, \cdot) = 0$ must also be imposed, since the quasistationary density is absorbed on the boundary.

In general it is not easy to solve the partial differential equation (5.7) on the half-plane $X^1 \geq 0$, subject to these boundary conditions. Our treatments of the generic $\mu < 1$ and generic $\mu > 1$ cases, in Sections 6 and 7 respectively, will be crafted to circumvent this problem. For the case $\mu < 1$ we shall expand on a larger lengthscale than $\mathcal{O}(\epsilon^{1/2})$; for the case $\mu > 1$, on which we have less information, we shall use stochastic analysis. In advance of our detailed treatments, we observe that the *far-field* behavior of the exit location density p_ϵ (on the $\mathcal{O}(\epsilon^{1/2})$ lengthscale near H) follows from (5.12)–(5.14). By (2.3) the exit location density is simply proportional to the normal derivative of the inner approximation v_ϵ^0. If we substitute the above expressions for $\boldsymbol{Z}(H)$, $\widehat{\boldsymbol{Z}}(H)$ and $\widehat{Z}_{\partial\Omega}(H)$ into (5.12)–(5.14), we obtain far-field asymptotics

$$p_\epsilon(s) \sim \begin{cases} \exp\left[0 \cdot (s^2/\epsilon)\right], & s/\epsilon^{1/2} \to +\infty; \\ \exp\left[-\dfrac{\mu(\mu+1)^2}{c^2 + (\mu+1)^2}(s^2/\epsilon)\right], & s/\epsilon^{1/2} \to -\infty \end{cases} \tag{5.15a}$$

if $\mu < 1$ (Subcase A), and

$$p_\epsilon(s) \sim \begin{cases} \exp\left[0 \cdot (s^2/\epsilon)\right], & s/\epsilon^{1/2} \to +\infty; \\ \exp\left[-\mu(s^2/\epsilon)\right], & s/\epsilon^{1/2} \to -\infty \end{cases} \tag{5.15b}$$

if $\mu < 1$ (Subcase B), and

$$p_\epsilon(s) \sim \begin{cases} \exp\left[-\dfrac{\mu(\mu-1)^2}{c^2+(\mu-1)^2}(s^2/\epsilon)\right], & s/\epsilon^{1/2} \to +\infty; \\ \exp\left[-\mu(s^2/\epsilon)\right], & s/\epsilon^{1/2} \to -\infty \end{cases} \tag{5.15c}$$

if $\mu > 1$. The zero coefficients in the exponents of (5.15a) and (5.15b) indicate that the corresponding asymptotics are sub-Gaussian. We have written s for Δx^2 (the distance along $\partial\Omega$, measured from H), for consistency with the Introduction, and have taken the wedge side of H to be the side on which $s < 0$. Notice that as $\mu \uparrow 1$ (resp. $\mu \downarrow 1$) the asymptotics of (5.15b) and (5.15c) come into agreement. Subcase A, however, has no $\mu > 1$ counterpart.

Actually, there is one nongeneric case in which the partial differential equation (5.7), subject to the boundary conditions (5.12)–(5.14), can be solved explicitly. This is the case when $c = 0$, *i.e.*, when the linearized drift $\boldsymbol{B}(H)$ at the saddle point has the property that its eigenvalues $\boldsymbol{e}_s$ and $\boldsymbol{e}_u$ are orthogonal with respect to the inner product specified by the local diffusivity tensor $\boldsymbol{D}(H)$. If $c = 0$ and $\mu > 1$, the classically forbidden wedge *vanishes*: the rays $\boldsymbol{e}_s$ and $\tilde{\boldsymbol{e}}_u$, which form the boundary of the wedge, become identical. In picturesque language, as $c \to 0$ (when $\mu > 1$) the wedge disappears into the boundary $\partial\Omega$, and the action becomes twice continuously differentiable on a neighborhood of the saddle point. In this case it follows from (5.15c), by setting $c = 0$, that the two Gaussian decay rates of the asymptotic exit location density are equal. This suggests that p_ϵ is asymptotic to a Gaussian. We now explain why this is the case.

If there is no wedge, the far-field asymptotics become Gaussian rather than piecewise Gaussian; they reduce to $\rho(X^1, X^2) \sim \exp\left(-\boldsymbol{X}^t\boldsymbol{Z}(H)\boldsymbol{X}/2\right)$, since only (5.12) applies. But if $c = 0$ the expression (5.9) for the matrix $\boldsymbol{Z}(H)$, which is valid when $\mu > 1$, simplifies to

$$\boldsymbol{Z}(H) = \begin{bmatrix} -2 & 0 \\ 0 & 2\mu \end{bmatrix}. \tag{5.16}$$

So the far-field asymptotics which must be imposed on the solution of (5.7) simplify greatly; we have $\rho(X^1, X^2) \sim \exp[(X^1)^2 - \mu(X^2)^2]$. Moreover if $c = 0$ the final term in (5.7) vanishes, allowing a solution on $X^1 \geq 0$ with these asymptotics to be found by separation of variables. It is

$$\rho(X^1, X^2) = \exp\left[-\mu(X^2)^2\right] G(X^1), \tag{5.17}$$

in which the boundary layer function $G(\cdot)$ is defined by

$$G(z) = e^{z^2}\,\mathrm{erf}(z) = \frac{2}{\sqrt{\pi}}e^{z^2}\int_{s=0}^{z} e^{-s^2}\,ds. \tag{5.18}$$

Therefore when $c = 0$, and $\mu > 1$, we have the inner approximation

$$v_\epsilon^0(x^1, x^2) \sim \{K(H)\exp\left(-W(H)/\epsilon\right)\}\exp\left[-\mu(x^2-H^2)^2/\epsilon\right] G\left((x^1-H^1)/\epsilon^{1/2}\right). \tag{5.19}$$

The factor $K(H)\exp\left(-W(H)/\epsilon\right)$ is included to facilitate matching with the outer approximation.

Note that in (5.19) we must interpret x^1-H^1, x^2-H^2 as linearly transformed ('primed') versions of the original coordinates x^1-H^1, x^2-H^2. $\boldsymbol{X} = (X^1, X^2)$ in (5.17) really means

$\boldsymbol{X}' = \boldsymbol{O}\boldsymbol{D}(H)^{-1/2}\boldsymbol{X}$, for $\boldsymbol{O}$ a suitably chosen (orthogonal) rotation matrix; similarly, $\boldsymbol{x}-H$ in (5.19) must be interpreted as $\boldsymbol{O}\boldsymbol{D}(H)^{-1/2}(\boldsymbol{x}-H)$. Using (5.16), we can rewrite (5.19) in a partially covariant form. We obtain

$$\begin{aligned}(5.20)\qquad & v_\epsilon^0(x^1,x^2) \sim \\ & \{K(H)\exp\left(-W(H)/\epsilon\right)\}\exp\left[-(x^i-H^i)W_{,ij}(H)(x^j-H^j)/2\epsilon\right] \\ & \quad \times \operatorname{erf}\left[(x^1-H^1)/\epsilon^{1/2}\right],\end{aligned}$$

with the same proviso on the interpretation of the factor x^1-H^1 in the argument of the error function. This way of writing the inner approximation to v_ϵ^0 makes it clear that its leading asymptotics as $\boldsymbol{x}/\epsilon^{1/2}\to\infty$ are indeed those of (5.1). The final factor in (5.20) is attributable to the absorbing boundary condition at $X^1=0$. This boundary layer factor may be written in fully covariant form as

$$(5.21)\qquad \operatorname{erf}\left(\lambda_u(H)^{1/2}n^iD_{ij}(H)(x^j-H^j)/\epsilon^{1/2}\right)$$

where n^i is a contravariant unit normal vector to $\partial\Omega$ at H, satisfying $n^iD_{ij}(H)t^j=0$ for any vector t^i tangent to $\partial\Omega$ at H, and normalized so that $n^iD_{ij}(H)n^j=1$. We have included in the argument of the error function a factor $\lambda_u(H)^{1/2}$, which will be present if $\lambda_u(H)$ is not taken to equal unity.

We stress that we can construct such a simple inner approximation as (5.20) in the case $\mu>1$ *only* when $c=0$, *i.e.*, only when the eigenvectors of $\boldsymbol{B}(H)$ are orthogonal with respect to the inner product specified by $D_{ij}(H)$. A covariant way of expressing this condition may be derived as follows. ${\boldsymbol{e}_s}^iD_{ij}{\boldsymbol{e}_u}^j=0$, *i.e.*, $\boldsymbol{e}_s^t\boldsymbol{D}(H)^{-1}\boldsymbol{e}_u=0$, means that $\boldsymbol{D}(H)^{-1/2}\boldsymbol{e}_s$ and $\boldsymbol{D}(H)^{-1/2}\boldsymbol{e}_u$ are orthogonal in the conventional sense. Equivalently, $\boldsymbol{D}(H)^{-1/2}\boldsymbol{B}(H)\boldsymbol{D}(H)^{1/2}$ has orthogonal eigenvectors and is a symmetric matrix. But $\boldsymbol{D}(H)^{-1/2}\boldsymbol{B}(H)\boldsymbol{D}(H)^{1/2}$ is symmetric if and only if $\boldsymbol{B}(H)\boldsymbol{D}(H)$ is symmetric, *i.e.*, if the tensor ${b^i}_{,j}D^{jk}$ is symmetric under the interchange of i and k at $\boldsymbol{x}=H$. This is the covariant form of the condition. It is easily checked that if $b^i=-D^{ij}\partial_j\Phi$ for some potential field Φ that has a saddle point at H, then the condition is necessarily satisfied. The $c=0$ condition for the validity of the inner approximation (5.20), when $\mu>1$, is really a condition that the drift $\boldsymbol{b}$ be *locally gradient* at H.

Stochastic exit models in which this local gradient condition holds are unfortunately nongeneric. But if $\mu>1$, and the condition holds, it is an easy matter to determine both the asymptotics of the exit location density on $\partial\Omega$, and the MFPT asymptotics. Equation (2.3) yields

$$(5.22)\qquad p_\epsilon(\boldsymbol{x}) \propto \exp\left[-(x^i-H^i)W_{,ij}(H)(x^j-H^j)/2\epsilon\right],\qquad \boldsymbol{x}\in\partial\Omega$$

for the density of the exit location distribution in the $\epsilon\to0$ limit, on the $\mathcal{O}(\epsilon^{1/2})$ lengthscale near H. So the density on $\partial\Omega$ is indeed asymptotically Gaussian, with the same falloff rate as $(\boldsymbol{x}-H)/\epsilon^{1/2}\to\infty$ to either side of the saddle point. We stress that this Gaussian behavior can only occur in the absence of a classically forbidden wedge.

Equation (2.7), which expresses $\lambda_\epsilon^{(0)}$ in terms of the flux of probability into $\partial\Omega$ near H, when applied to the inner approximation (5.20) will yield

$$(5.23)\quad (E\tau_\epsilon)^{-1} \sim \lambda_\epsilon^{(0)} \sim \frac{1}{\pi}\sqrt{\det \boldsymbol{Z}(S)}\sqrt{\frac{\lambda_u(H)}{|\lambda_s(H)|}}K(H)\exp\left(-W(H)/\epsilon\right),\quad \epsilon\to0,$$

as the weak-noise MFPT asymptotics. Here the factor $\sqrt{\det \boldsymbol{Z}(S)}$ arises from the denominator of (2.7). The asymptotics of (5.23) are valid only if the coordinates x^i near H have been linearly transformed in such a way that $\boldsymbol{D}(H) = \boldsymbol{I}$; this was assumed when we derived the inner approximation (5.20).

$$(5.24)\quad (E\tau_\epsilon)^{-1} \sim \lambda_\epsilon^{(0)} \sim \frac{\lambda_u(H)}{\pi}\sqrt{\frac{\det \boldsymbol{Z}(S)}{|\det \boldsymbol{Z}(H)|}} K(H) \exp\left(-W(H)/\epsilon\right), \qquad \epsilon \to 0$$

is the generalization to arbitrary coordinate systems.

We know from Wentzell-Freidlin theory that the leading order growth of the MFPT $E\tau_\epsilon$ in the $\epsilon \to 0$ limit is exponential, with rate constant $W(H)$. The asymptotic expression (5.24) includes this exponential growth, and also a constant pre-exponential factor. The pre-exponential factor, like $W(H)$, is nonlocal: it is not uniquely determined by the behavior of the stochastic model in the vicinity of S and H. That is because the 'frequency factor' $K(H)$, which multiplies the frequency of excursions to the vicinity of H, can only be computed by integrating the system of ordinary differential equations (3.8a), (3.8b), (3.11), (3.12), (3.14) from S to H along the MPEP. The only exception to this is when $b^i = -D^{ij}\partial_j\Phi$ for some differentiable function Φ, *i.e.*, when $\boldsymbol{b}$ is globally as well as locally gradient. In this case it is easily checked that $W = 2\Phi$ and $K \equiv 1$, so the pre-exponential factor in (5.24) is locally determined.

The $\epsilon \to 0$ asymptotics which we have just derived for the exit location density p_ϵ and the MFPT $E\tau_\epsilon$ are quite familiar from the literature [27, 42, 46, 50]. In fact the MFPT formula (5.24) can, in the context of chemical physics, be traced back to Eyring [21]. But our new derivation of the Eyring formula makes it clear that it is valid without qualification *only* when the classically forbidden wedge is absent. In general this will occur only in a single nongeneric case: when the drift field near H satisfies the local gradient condition, and moreover the eigenvalue ratio $\mu > 1$ (*i.e.*, $\partial_i b^i(H) < 0$). This has not previously been realized.

6. Skewing and MFPT asymptotics when $\partial_i b^i(H) > 0$. We now turn to generic models with $b^i{}_{,i}(H) > 0$, *i.e.*, models in which the eigenvalue ratio $\mu = |\lambda_s(H)|/\lambda_u(H) < 1$. By building on the analysis of Sections 4 and 5, we shall show that generically, the limiting exit location distribution near the saddle point H is a Weibull distribution on the $\mathcal{O}(\epsilon^{\mu/2})$ lengthscale, as mentioned in the Introduction. It is non-Gaussian and asymmetric.

In this section we shall for simplicity take the linearized drift $B^i{}_j(H) = b^i{}_{,j}(H)$ to be

$$(6.1)\qquad \boldsymbol{B}(H) = \begin{bmatrix} \lambda_u(H) & 0 \\ c & \lambda_s(H) \end{bmatrix} = \begin{bmatrix} 1 & 0 \\ c & -\mu \end{bmatrix},$$

as in Section 5, and take $\boldsymbol{D}(H) = \boldsymbol{I}$. The lower triangular form for $\boldsymbol{B}(H)$ can be arranged by an appropriate linear change of coordinates near H, as can $\boldsymbol{D}(H) = \boldsymbol{I}$. $\lambda_u(H) = 1$ can be arranged by a rescaling of time and noise strength. With this choice of $\boldsymbol{B}(H)$, the boundary $\partial\Omega$ will (near H) be parallel to the x^2-axis. The most probable exit path (MPEP) from S to H will generically be tangent to $\partial\Omega$, and without loss of generality we assume that it approaches H from the first quadrant, as in Fig. 4.1(a).

The basic properties of $\mu < 1$ models were worked out in Sections 4 and 5. Generically there is a classically forbidden wedge emanating from H, on the boundary of which the Hessian matrix $W_{,ij}$ is discontinuous. If $c < 0$ ('Subcase A') then within the wedge $W_{,ij}(\boldsymbol{x})$ has rank-1 limit $\widehat{W}_{,ij}(H)$ as $\boldsymbol{x} \to H$, though if $c > 0$ ('Subcase B') $W(\boldsymbol{x})$ in the wedge will not be a quadratic function of $\boldsymbol{x}$ near H. If $\boldsymbol{x} \to H$ from outside the wedge, *e.g.*, along the MPEP, then $W_{,ij}(\boldsymbol{x}) \to 0$. Outside the wedge the action W is 'flat' near H. Since the outer approximation to the quasistationary density $v_\epsilon^0(\boldsymbol{x})$ contains an exponential factor $\exp\left(-W(\boldsymbol{x})/\epsilon\right)$, this is a sign that on the classically allowed side of H, the quasistationary density falls off only slowly (more slowly than quadratically). As a consequence the appropriate lengthscale for an inner approximation near H should be larger than $\mathcal{O}(\epsilon^{1/2})$. On the $\mathcal{O}(\epsilon^{1/2})$ lengthscale the asymptotics of v_ϵ^0 and the exit location density p_ϵ are given by (5.12)–(5.14) and (5.15a)–(5.15b), but an approximation on that lengthscale is not particularly useful.

We showed in Section 4 that when $\mu < 1$, the tangent space $T_{(H,0)}\mathcal{M}^u_{(S,0)}$ to the manifold $\mathcal{M}^u_{(S,0)} \subset \bar\Omega \times \mathbb{R}^2$ at $(H,0)$ generically equals the linear span of two eigenvectors of the linearized Hamiltonian flow: the stable eigenvector $(\boldsymbol{e}_s, 0)$ and the unstable eigenvector $(\boldsymbol{e}_u, 0)$. Since the MPEP $\boldsymbol{q}^*$, regarded as a trajectory in the phase space $\bar\Omega \times \mathbb{R}^2$, terminates at $(H,0)$, it must approach $(H,0)$ along the tangent vector $(\boldsymbol{e}_s, 0)$; since $\boldsymbol{e}_s$ lies in $\partial\Omega$, that is why the MPEP is tangent to $\partial\Omega$. This tangency condition is of course an asymptotic statement, valid only as $t \to \infty$, *i.e.*, as $(H,0)$ is approached. A more refined analysis would take into account the fact that the linearization of the Hamiltonian flow has both $(\boldsymbol{e}_s, 0)$ and $(\tilde{\boldsymbol{e}}_s, \tilde{\boldsymbol{g}}_s)$ as stable eigenvectors. They have eigenvalues $\lambda_s(H) = -\mu$ and $-\lambda_u(H) = -1$ respectively, so a precise description of the $t \to \infty$ asymptotics of the MPEP would be

$$\boldsymbol{q}^*(t) \sim H + C_s e^{-\mu t}\boldsymbol{e}_s + \tilde{C}_s e^{-t}\tilde{\boldsymbol{e}}_s, \qquad t \to \infty. \tag{6.2}$$

Since $\mu < 1$, the first term is dominant as $t \to \infty$, and gives rise to the approach along $\partial\Omega$. But the coefficient $\tilde{C}_s$ of the subdominant term, like C_s, is generically nonzero. The two coefficients can only be found by computing the MPEP explicitly: by integrating Hamilton's equations (3.8) from $(\boldsymbol{x}, \boldsymbol{p}) = (S, 0)$ at $t = -\infty$ to $(H, 0)$ at $t = \infty$. The fact that $\tilde{C}_s$ is generically nonzero was taken into account when plotting Figs. 4.1(a), 4.2(a), and 4.2(b); in those three figures, the slight deviation of the approaching MPEP from $\partial\Omega$ is due to the $\tilde{\boldsymbol{e}}_s$ term.

Explicit formulæ for the eigenvectors $\boldsymbol{e}_s$ and $\tilde{\boldsymbol{e}}_s$ appear in (5.8); we may take $\boldsymbol{e}_s = (0,1)$ and $\tilde{\boldsymbol{e}}_s = (\mu - 1, c)$. So (6.2) may be written, if $\Delta\boldsymbol{x}$ signifies $\boldsymbol{x} - H$, as

$$(\Delta x^1, \Delta x^2) \sim \left(\tilde{C}_s(\mu-1)e^{-t}, C_s e^{-\mu t} + \tilde{C}_s c e^{-t}\right). \tag{6.3}$$

We must have $\tilde{C}_s < 0$ and $C_s > 0$, since it is our convention that the MPEP approaches H from the first quadrant. As $t \to \infty$ and H is approached, the MPEP will generically be asymptotic to the curve $\Delta x^2 = A(\Delta x^1)^\mu$, where $A \stackrel{\text{def}}{=} C_s[\tilde{C}_s(\mu-1)]^{-\mu}$. This asymptotic behavior occurs irrespective of the value of c.

Since the boundary layer near the characteristic boundary $\partial\Omega$ has thickness $\mathcal{O}(\epsilon^{1/2})$, the inner approximation near H should be valid when $\Delta x^1 = \mathcal{O}(\epsilon^{1/2})$. But if the inner approximation is to be valid on a region containing a nontrivial (as $\epsilon \to 0$) portion of the MPEP, it should also be valid when $\Delta x^2 = \mathcal{O}(\epsilon^{\mu/2})$. So $x^1 - H^1$ and $x^2 - H^2$ should be treated *asymmetrically*: When $\mu < 1$, the appropriate boundary region for the inner approximation is a strip near $\partial\Omega$ on which $\Delta x^1 \ll \Delta x^2$. This thin strip should extend from H along $\partial\Omega$ in the direction of the approaching MPEP; equivalently, it should *not* extend in the direction of the forbidden wedge. As previously discussed, the appropriate lengthscale for an inner approximation on the wedge side of H is $\mathcal{O}(\epsilon^{1/2})$, not $\mathcal{O}(\epsilon^{\mu/2})$.

Let us write (x, z) for $\left(\Delta x^1, (\Delta x^2)^{1/\mu}\right)$; the change to noncovariant notation will emphasize the asymmetry. In the (x,z)-plane the boundary region will be the region where $x,\, z = \mathcal{O}(\epsilon^{1/2})$. The MPEP will approach $H = (0,0)$ as $t \to \infty$ along an asymptotically linear trajectory $z \sim A^{1/\mu}x$. It is an easy exercise to show, using the matrix Riccati equation (3.14) in the linear approximation near H, that irrespective of the asymptotic slope $A^{1/\mu}$, the matrix of second derivatives

$$\widetilde{\boldsymbol{Z}}(x,z) \stackrel{\text{def}}{=} \begin{bmatrix} \dfrac{\partial^2 W}{\partial x^2} & \dfrac{\partial^2 W}{\partial x \partial z} \\ \dfrac{\partial^2 W}{\partial z \partial x} & \dfrac{\partial^2 W}{\partial z^2} \end{bmatrix} \tag{6.4}$$

will have a finite (nonzero) limit as $t \to \infty$, *i.e.*, as the MPEP approaches H. In the complement of the forbidden wedge, the action W near H is quadratic in x and z.

This quadratic leading-order behavior will mandate far-field $[(x,z)/\epsilon^{1/2} \to \infty]$ asymptotics for the inner approximation to v_ϵ^0 that are Gaussian in terms of x and z. The inner approximation is best written in terms of the stretched variables $X = x/\epsilon^{1/2}$ and $Z = z/\epsilon^{1/2}$. It may be constructed by solving a linearized version of the approximate forward Kolmogorov equation $\mathcal{L}_\epsilon^* \rho = 0$, as follows. In the linear approximation we take $b^i(\boldsymbol{x}) \approx B^i{}_j(H)(x^j - H^j)$ and $D^{ij}(\boldsymbol{x}) \approx D^{ij}(H)$, and the Kolmogorov equation reduces to

$$(\epsilon/2)D^{ij}(H)\partial_i\partial_j\rho - \partial_i[B^i{}_j(H)(x^j - H^j)\rho] = 0. \tag{6.5}$$

Substituting both (6.1) and $\boldsymbol{D}(H) = \boldsymbol{I}$, and changing variables from (x^1, x^2) to $X = (x^1 - H^1)/\epsilon^{1/2}$ and $Y = (x^2 - H^2)/\epsilon^{\mu/2}$, yields

$$\frac{1}{2}\frac{\partial^2 \rho}{\partial X^2} + \frac{\epsilon^{1-\mu}}{2}\frac{\partial^2 \rho}{\partial Y^2} - \frac{\partial}{\partial X}[X\rho] + \mu\frac{\partial}{\partial Y}[Y\rho] - c\epsilon^{(1-\mu)/2}\frac{\partial}{\partial Y}[X\rho] = 0. \tag{6.6}$$

In the $\epsilon \to 0$ limit this becomes

$$\frac{1}{2}\frac{\partial^2 \rho}{\partial X^2} - \frac{\partial}{\partial X}[X\rho] + \mu\frac{\partial}{\partial Y}[Y\rho] = 0, \tag{6.7}$$

and substituting $Y = Z^\mu$ yields

$$\frac{1}{2}\frac{\partial^2 \rho}{\partial X^2} - X\frac{\partial \rho}{\partial X} + Z\frac{\partial \rho}{\partial Z} - (1-\mu)\rho = 0. \tag{6.8}$$

This PDE for $\rho = \rho(X, Z)$ must be solved in the boundary region.

In terms of the stretched variables (X, Z) we may view the boundary region as the right-half plane $X \geq 0$, and the boundary $\partial\Omega$ as the Z-axis. The location of the classically forbidden wedge, in terms of X and Z, is easily determined. As shown in Section 4 the wedge is bounded by the ray consisting of all multiples of $\boldsymbol{e}_u$; since $\boldsymbol{e}_u = (\mu+1, c)$ by (5.8b), its boundary has equation $\Delta x^2 = [c/(\mu+1)]\Delta x^1$, or $Z = [c/(\mu+1)]^{1/\mu}\epsilon^{(1-\mu)/2\mu}X^{1/\mu}$. In the $\epsilon \to 0$ limit the boundary of the wedge becomes the X-axis: of the first and fourth quadrants in the (X, Z)-plane one is classically allowed, and the other is forbidden. We are taking the MPEP to approach $(X, Z) = (0, 0)$ from the first quadrant, so it is the fourth that is forbidden. So (6.8) should be solved only in the first quadrant. The extreme suppression of the quasistationary density in the forbidden wedge (on the $\mathcal{O}(\epsilon^{\mu/2})$ lengthscale) allows us to set $\rho = 0$ when $Z \leq 0$, for both Subcase A and Subcase B.

A family of solutions of equation (6.8), each with far-field asymptotics that are Gaussian in X and Z, can be found by inspection. Each solution is of the form

$$\rho(X, Z) \propto \begin{cases} Z^{1-\mu}\exp(2BXZ - B^2Z^2), & \text{if } Z > 0; \\ 0, & \text{if } Z \leq 0, \end{cases} \tag{6.9}$$

for some constant B. Actually we shall use antisymmetrized (odd) versions of these solutions, since ρ must satisfy the Dirichlet boundary condition $\rho(0, \cdot) = 0$ on account of absorption of probability on $\partial\Omega$. Antisymmetrizing under $X \mapsto -X$ yields

$$\rho(X,Z) \propto \begin{cases} Z^{1-\mu}\sinh(2BXZ)\exp(-B^2Z^2), & \text{if } Z>0; \\ 0, & \text{if } Z \le 0. \end{cases} \tag{6.10}$$

Rewriting (6.10) in terms of $\Delta x^i = x^i - H^i$ gives

$$v_\epsilon^0(\boldsymbol{x}) \sim \begin{cases} C(\Delta x^2)^{(1/\mu)-1}\sinh\left[2B(\Delta x^1)(\Delta x^2)^{1/\mu}/\epsilon\right]\exp\left[-B^2(\Delta x^2)^{2/\mu}/\epsilon\right], & \Delta x^2>0; \\ 0, & \Delta x^2 \le 0 \end{cases} \tag{6.11}$$

as the desired inner approximation for the case $\mu<1$, with C to be found by matching to the outer approximation. From (6.11) we can read off the behavior of W and K as $\boldsymbol{x}\to H$ when $\Delta x^2>0$ (*i.e.*, in the complement of the forbidden wedge). Necessarily

$$W(\boldsymbol{x}) \sim -2B(\Delta x^1)(\Delta x^2)^{1/\mu} + B^2(\Delta x^2)^{2/\mu} \tag{6.12a}$$

$$K(\boldsymbol{x}) \sim C(\Delta x^2)^{(1/\mu)-1}. \tag{6.12b}$$

It is a useful exercise to verify that the leading-order approximations (6.12), irrespective of the value of B, are consistent with the system of ordinary differential equations (3.8a), (3.8b), (3.11), (3.12), (3.14) in the linear approximation near H.

Notice that $K\to 0$ as $\boldsymbol{x}\to H$ from outside the wedge: in particular, along the MPEP. In other words, our analysis predicts that the nominal frequency factor $K(H)$ is *generically zero* when $\mu<1$. This phenomenon has in fact been seen in numerical studies of particular models (see, *e.g.*, Ref. [6]). We have verified that this behavior is generic by numerically integrating the transport equation (3.12), in a wide variety of models with $\mu<1$, from $(\boldsymbol{x},\boldsymbol{p})=(S,0)$ to $(H,0)$. The fact that $K(H)=0$ is yet another reason why the traditional formula (5.24) for the MFPT asymptotics cannot be generically applicable.

It turns out that the model-dependent constant B in the inner approximation is uniquely determined by the approach path taken by the MPEP. Since $p_i=\partial_i W$, differentiation of (6.12a) yields

$$\boldsymbol{p}(H+\Delta\boldsymbol{x}) \sim \left(-2B(\Delta x^2)^{1/\mu}, -2B\mu^{-1}(\Delta x^1)(\Delta x^2)^{(1/\mu)-1} + 2B^2\mu^{-1}(\Delta x^2)^{(2/\mu)-1}\right) \tag{6.13}$$

on the $\Delta x^2 = O\left((\Delta x^1)^\mu\right)$ lengthscale near H. But by (6.1),

$$\boldsymbol{b}(H+\Delta\boldsymbol{x}) \approx (\Delta x^1, -\mu\,\Delta x^2 + c\,\Delta x^1) \tag{6.14}$$

near H. Substituting (6.13)–(6.14) into Hamilton's equation (3.8a) for $\dot{\boldsymbol{x}}$ yields, to leading order,

$$\frac{d}{dt}(\Delta x^1,\Delta x^2) \sim \left(-2B(\Delta x^2)^{1/\mu} + \Delta x^1, -\mu\,\Delta x^2\right). \tag{6.15}$$

It is trivial to verify that this asymptotic equation of motion near H is compatible with the MPEP approach path $\Delta x^2 \sim A(\Delta x^1)^\mu$ if and only if $B=A^{-1/\mu}$. Since A is the limit of the ratio $\Delta x^2/(\Delta x^1)^\mu$ along the MPEP as it approaches H, the constant B in the inner approximation may be computed numerically, if desired.

Now that we have constructed an inner approximation to the quasistationary density v_ϵ^0 that is asymptotically accurate as $\epsilon\to 0$, we can compute the asymptotic exit location distribution and MFPT asymptotics. Since $\boldsymbol{D}(H)=\boldsymbol{I}$, equation (2.3) says that asymptotically, the density of the exit location measure on $\partial\Omega$ is proportional to the normal derivative of v_ϵ^0. This is simply the rate at which probability is absorbed on $\partial\Omega$, as a function of position. By differentiating the inner approximation (6.11) with respect to Δx^1 and setting Δx^1 to zero we obtain (since $B = A^{-1/\mu}$)

$$p_\epsilon(s) \sim \begin{cases} \left(\dfrac{2}{\mu A^{2/\mu}\epsilon}\right) s^{(2/\mu)-1} \exp[-(s/A)^{2/\mu}/\epsilon], & s > 0; \\ 0, & s \le 0. \end{cases} \tag{6.16}$$

Here we have written s for Δx^2 (the distance along $\partial\Omega$, measured from H) for consistency with the Introduction and Section 5. The overall normalization of (6.16) is fixed by the condition that p_ϵ have unit total mass.

The asymptotic exit location density (6.16), which is localized on the $s = \mathcal{O}(\epsilon^{\mu/2})$ lengthscale, is of an unusual form. It is the density of a Weibull distribution [3], with shape parameter $2/\mu$ and scale parameter $1/A\epsilon^{\mu/2}$. Weibull-distributed random variables are simply powers of exponential random variables, and p_ϵ may be viewed as the density of an 'offset' random variable $\mathfrak{S}_\epsilon$ equal to $AM^{\mu/2}$, where M is an exponential variate of mean ϵ. The Weibull distribution is decidedly 'skewed'; in fact it is supported entirely on the $s > 0$ side of the saddle point. That $s > 0$, rather than $s < 0$, appears here is solely a matter of convention. By convention the $s > 0$ side of H is the side from which the MPEP approaches, as in Fig. 4.1(a). For later use we note that

$$E\mathfrak{S}_\epsilon = \int_0^\infty s\, p_\epsilon(s)\, ds \sim A\Gamma(1+\mu/2)\epsilon^{\mu/2}, \quad \epsilon \to 0 \tag{6.17}$$

is the expected offset from H along $\partial\Omega$, in models with $\mu < 1$, at the time of exit.

The qualitative features of the asymptotic density (6.16) can be explained by reference to Fig. 4.1(a). The quantity $s^{2/\mu}$ in the exponent is roughly proportional to the square of the distance between the point $(0, s)$ on $\partial\Omega$ and the closest point on the approaching MPEP. This is consistent with a picture developed elsewhere [34], according to which the MPEP is surrounded by a 'tube' of probability current, the tube having a Gaussian transverse profile. We have already discussed why the limiting $p_\epsilon(s)$, on the $\mathcal{O}(\epsilon^{\mu/2})$ lengthscale, is zero for $s < 0$. The points on $\partial\Omega$ with $s < 0$ are classically forbidden, and $p_\epsilon(s)$ in the forbidden region falls to zero on the $s = \mathcal{O}(\epsilon^{1/2})$ lengthscale, as summarized in (5.15a)–(5.15b). Subcases A and B differ significantly on the $\mathcal{O}(\epsilon^{1/2})$ lengthscale, but on the larger $\mathcal{O}(\epsilon^{\mu/2})$ lengthscale their behavior is identical.

It is clear how the $\epsilon \to 0$ MFPT asymptotics may be computed from the inner approximation (6.11). Asymptotically $\lambda_\epsilon^{(0)}$, *i.e.*, $(E\tau_\epsilon)^{-1}$, is simply the flux of probability into $\partial\Omega$. As such it is proportional to the constant prefactor C in (6.11). If the inner approximation is to match to the outer approximation, by (6.12b) we must have

$$C = L \exp\left(-W(H)/\epsilon\right), \tag{6.18}$$

where L is the limit of the quantity $K(\boldsymbol{x})/(\Delta x^2)^{(1/\mu)-1}$ as $\boldsymbol{x} \to H$ along the MPEP. This formula for C has novel consequences. The factor $\exp\left(-W(H)/\epsilon\right)$ gives rise to the familiar Wentzell-Freidlin growth factor in $E\tau_\epsilon$. But the pre-exponential factor in the asymptotics of $(E\tau_\epsilon)^{-1}$ is *not* proportional to the (generically zero) nominal frequency factor $K(H)$, as in the Eyring formula (5.24), but rather to L, the rate at which $K(\boldsymbol{x})$ approaches zero as the MPEP approaches H. In fact substituting the inner approximation into (2.7), and using $B = A^{-1/\mu}$, yields

$$(E\tau_\epsilon)^{-1} \sim \lambda_\epsilon^{(0)} \sim \frac{\mu A^{1/\mu} L}{4\pi}\sqrt{\det \boldsymbol{Z}(S)}\exp\left(-W(H)/\epsilon\right), \qquad \epsilon \to 0 \tag{6.19}$$

as the replacement for the Eyring formula (5.24) when $\mu < 1$. The $\sqrt{\det \boldsymbol{Z}(S)}$ factor arises from the denominator of (2.7), as in (5.24). We remind the reader that we are assuming $\lambda_u(H) = 1$ and $\boldsymbol{D}(H) = \boldsymbol{I}$ here.

The generic applicability (when $\mu < 1$) of this formula for the MFPT asymptotics, and the generic *inapplicability* of the traditional formula (5.24), have not previously been recognized. It is remarkable that despite the nominal frequency factor $K(H)$ equalling zero, the pre-exponential factor in (6.19) fails to be ϵ-dependent. Naively one would have expected it to contain a positive power of ϵ. A positive power of ϵ is known to occur in the weak-noise reciprocal MFPT asymptotics of stochastic models where the frequency factor equals zero on account of the exit location on $\partial\Omega$ converging to an unstable fixed point [32].

7. Skewing when $\partial_i b^i(H) < 0$. We now turn to generic models with $b^i{}_{,i}(H) < 0$, *i.e.*, models in which the eigenvalue ratio $\mu = |\lambda_s(H)|/\lambda_u(H) > 1$. The asymptotic exit location distribution near the saddle point H is localized on the $\mathcal{O}(\epsilon^{1/2})$ lengthscale, and we showed in Section 5 that it is generically non-Gaussian: It has different Gaussian falloff rates to either side of H. In this section we shall work out an algorithm for computing its moments of any desired order, though we shall not compute an explicit expression for its density. Our algorithm will be based on a stochastic analysis, rather than on the construction of an inner approximation to the quasistationary probability density.

As in Sections 5 and 6, without loss of generality take $\boldsymbol{D}(H) = \boldsymbol{I}$. Also take $\lambda_u = 1$, and take the linearized drift $\boldsymbol{B}(H) = [b^i{}_{,j}(H)]$ to be of the form

$$\boldsymbol{B}(H) = \begin{bmatrix} \lambda_u(H) & 0 \\ c & \lambda_s(H) \end{bmatrix} = \begin{bmatrix} 1 & 0 \\ c & -\mu \end{bmatrix}. \tag{7.1}$$

With this choice of $\boldsymbol{B}(H)$ the boundary $\partial\Omega$ near H will be parallel to the x^2-axis, as in Figs. 4.1 and 4.2. Also, translate coordinates so that $H = (0,0)$. With these normalizations the stochastic differential equation (1.1) becomes, in the linear approximation near H,

$$dx^1_\epsilon(t) = x^1_\epsilon(t)\,dt + \epsilon^{1/2} dw_1(t) \tag{7.2a}$$

$$dx^2_\epsilon(t) = -\mu x^2_\epsilon\,dt + c x^1_\epsilon(t)\,dt + \epsilon^{1/2} dw_2(t). \tag{7.2b}$$

If the ‘stretched’ process $t \mapsto (X(t), Y(t))$ in the (X,Y)-plane is defined to equal $\left(x^1_\epsilon(t), x^2_\epsilon(t)\right)/\epsilon^{1/2}$, these equations become

$$dX(t) = X\,dt + dw_1(t) \tag{7.3a}$$

$$dY(t) = -\mu Y\,dt + cX\,dt + dw_2(t). \tag{7.3b}$$

So $t \mapsto X(t)$ is an inverted (repelling) Ornstein-Uhlenbeck process. On the $\mathcal{O}(\epsilon^{1/2})$ lengthscale near H the region $\bar\Omega$ becomes the right-half plane $X \geq 0$, and the fact that equation (7.3a) does not involve Y indicates that with these normalizations, the exit problem is essentially one-dimensional.

Our interest is in the final approach to the boundary, which as $\epsilon \to 0$ will take place along the MPEP (most probable exit path) determined in Sections 4 and 5. Generically the MPEP, as shown in Fig. 4.1(b), is tangent to the stable ray $\tilde{\boldsymbol{e}}_s$ emanating from H. But as computed in (5.8c), $\tilde{\boldsymbol{e}}_s$ equals $(\mu-1, c)$, when the linearized drift $B^i{}_j(H)$ is of the form (7.1). So as $\epsilon \to 0$, the final approach to $\partial\Omega$, in the linear approximation near H, should be increasingly concentrated near the line $x^2/x^1 = c/(\mu-1)$. To be sure, on the $\mathcal{O}(\epsilon^{1/2})$ lengthscale the approach path will not have a deterministic limit as $\epsilon \to 0$. However, the straight-line deterministic asymptotics should appear in the *far field* of the $\mathcal{O}(\epsilon^{1/2})$ lengthscale: going backward in time from the boundary hitting time, the approach path should be asymptotic to the line $Y/X = c/(\mu-1)$.

The random variable $\mathfrak{S}_\epsilon \stackrel{\text{def}}{=} \epsilon^{1/2} Y(\tau_\epsilon)$, the displacement from H along the boundary $\partial\Omega$ at the hitting time τ_ϵ, is the quantity whose distribution we wish to compute. We can define a time-reversed process $\left(\tilde{X}(u), \tilde{Y}(u)\right)$ to equal $(X(\tau_\epsilon - u), Y(\tau_\epsilon - u))$, $u \geq 0$; τ_ϵ is of course a random variable, which depends on the sample path. With this definition, $\tilde{X}(0) = 0$ and $\tilde{Y}(0) = \mathfrak{S}_\epsilon/\epsilon^{1/2}$. We now explain how the small-ϵ asymptotics of the distribution of $\mathfrak{S}_\epsilon$ may be computed.

A straightforward integration of (7.3b) from $u = 0$ to $u = T$, *i.e.*, from $t = \tau_\epsilon$ to $t = \tau_\epsilon - T$, yields that for any $T > 0$,

$$\tilde{Y}(0) = \tilde{Y}(T) e^{-\mu T} + \int_0^T e^{-\mu u} [c \tilde{X}(u)\, du - dw_2(u)]. \tag{7.4}$$

We shall show shortly that as $\epsilon \to 0$, the expected transit time of the final approach path tends to infinity. This justifies the taking of the $T \to \infty$ limit when computing $\epsilon \to 0$ asymptotics. Taking the $T \to \infty$ limit yields

$$\tilde{Y}(0) \sim \int_0^\infty e^{-\mu u} [c \tilde{X}(u)\, du - dw_2(u)], \tag{7.5}$$

which is to be interpreted as a statement that the left and right-hand sides are distributed identically in the $\epsilon \to 0$ limit. But $\int_0^\infty e^{-\mu u} dw_2(u)\, du$ is a Gaussian random variable of mean zero and variance $1/2\mu$. It follows that as $\epsilon \to 0$, we have the *asymptotically accurate representation*

$$\mathfrak{S}_\epsilon/\epsilon^{1/2} \sim c\, \mathfrak{I}(\mu) + \mathfrak{Z}/\sqrt{2\mu}, \tag{7.6}$$

where $\mathfrak{Z}$ is standard normal and the integral

$$\mathfrak{I}(\mu) \stackrel{\text{def}}{=} \int_0^\infty e^{-\mu u} \tilde{X}(u)\, du \tag{7.7}$$

is a weighted area under the graph of the time-reversed process $\tilde{X}(u)$, $u \geq 0$. The two terms in the representation (7.6) are independent, and the asymptotic exit location density $p_\epsilon(s)$ equals $(d/ds)\,\Pr(\mathfrak{S}_\epsilon \leq s)$, the probability density of $\mathfrak{S}_\epsilon$.

When the off-diagonal drift coefficient c equals zero, we see from the above representation that there is no skewing: the exit location distribution is asymptotically Gaussian, with variance $\epsilon/(2\mu)$. Moreover, *the skewing of the exit location distribution when* $\mu > 1$ *is attributable to the asymmetry of the density of the random variable* $\mathfrak{I}(\mu)$. This conclusion meshes nicely with the results of Section 5. We deduced there that when $\mu > 1$, $p_\epsilon(s)$ has different Gaussian decay rates as $s/\epsilon^{1/2} \to \pm\infty$; from (5.15c),

$$p_\epsilon(s) \sim \begin{cases} \exp\left[-\dfrac{\mu(\mu-1)^2}{c^2 + (\mu-1)^2}(s^2/\epsilon)\right], & s/\epsilon^{1/2} \to +\infty; \\ \exp\left[-\mu(s^2/\epsilon)\right], & s/\epsilon^{1/2} \to -\infty. \end{cases} \tag{7.8}$$

In deriving (7.8) the convention was adopted that the MPEP should approach H from the $s \geq 0$ side; this amounts to assuming that $c \geq 0$. The Gaussian falloff of the density of the $\mathfrak{Z}/\sqrt{2\mu}$ term in (7.6) may be viewed as the cause of the comparatively rapid Gaussian decay of $p_\epsilon(s)$ as $s/\epsilon^{1/2} \to -\infty$, since the random variable $\mathfrak{I}(\mu)$ is non-negative. In fact by independence, the density $p_\epsilon(\cdot)$ will be the convolution of the densities of $\epsilon^{1/2}\mathfrak{I}(\mu)$ and $\epsilon^{1/2}\mathfrak{Z}/\sqrt{2\mu}$. Equivalently, the generic asymptotic exit location density on the $\mathcal{O}(\epsilon^{1/2})$

lengthscale will be the convolution of the density of $c\,\mathfrak{I}(\mu)$ with a Gaussian (the density of $\mathfrak{Z}/\sqrt{2\mu}$).

To determine the distribution of the random variable $\mathfrak{I}(\mu)$, or at least its moments, we need to analyse the process $u \mapsto \tilde{X}(u)$. Recall that this is a time-reversed, scaled version of the one-dimensional process $t \mapsto x^1_\epsilon(t)$, conditioned on its exit at time τ_ϵ. To facilitate the analysis, we shall impose a second conditioning. By the 'final approach path' we shall mean that segment of the trajectory $t \mapsto \boldsymbol{x}_\epsilon(t)$ which leaves some specified neighborhood of S and terminates on $\partial\Omega$ at time τ_ϵ. Let $a > 0$ be specified, and suppose that along the final approach path, $x^1_\epsilon(t)$ first reaches the point $x^1 = a\epsilon^{1/2}$ at time $t = \tau_\epsilon - \mathfrak{u}$; equivalently, that $X(t)$ first reaches the point $X = a$ at time $t = \tau_\epsilon - \mathfrak{u}$. Then the process $X(t)$, $\tau_\epsilon - \mathfrak{u} \le t \le \tau_\epsilon$, will be an inverted Ornstein-Uhlenbeck process conditioned to satisfy $X(\tau_\epsilon) = 0$ and $X(t) > 0$ for all $t \in (\tau_\epsilon - \mathfrak{u}, \tau_\epsilon)$. And the time-reversed process $\tilde{X}(u)$, $0 \le u \le \mathfrak{u}$, will be an Ornstein-Uhlenbeck process conditioned to satisfy $\tilde{X}(0) = 0$ and $\tilde{X}(u) > 0$ for all $u \in (0, \mathfrak{u})$.

Conditioned Ornstein-Uhlenbeck processes are well understood, so the only obstacle to a full understanding of the $\tilde{X}$ process is the need to determine the distribution of $\mathfrak{u}$, the 'additional time to exit' random variable. It is not difficult to compute the asymptotics of the distribution of $\mathfrak{u}$ in the large-a limit. The transition density $p(X_0, t_0; X_1, t_1)$ of an Ornstein-Uhlenbeck process is of the form

(7.9) $$p(X_0, t_0; X_1, t_1) = [2\pi\sigma^2_{t_1-t_0}]^{-1/2} \exp\left[-(X_1 - e^{t_1-t_0}X_0)^2/2\sigma^2_{t_1-t_0}\right]$$

where $\sigma^2_z \stackrel{\text{def}}{=} (e^{2z} - 1)/2$ is the variance at elapsed time z. If the process $X(t)$ is conditioned to begin at $a > 0$ at some specified time t_0, the probability of its having reached $X = 0$ by time $t_0 + \tilde{u}$ will by the method of images equal [11]

(7.10) $$2\left\{1 - \int_{X_1 \ge 0} p(a, t_0; X_1, t_0 + \tilde{u})\, dX_1\right\}.$$

This absorption probability equals $\Pr(\mathfrak{u} \le \tilde{u})$, the probability that the additional time to absorption is no greater than $\tilde{u}$. Substituting (7.9) into (7.10), plus some elementary manipulations, yields

(7.11) $$\Pr(\mathfrak{u} \le \tilde{u}) \sim \exp\left(-e^{-2(\tilde{u} - log a)}\right), \quad a \to \infty.$$

It follows that we may write

(7.12) $$\mathfrak{u} \sim \log a + \mathfrak{G}, \quad a \to \infty,$$

where the random variable $\mathfrak{G}$ satisfies

(7.13) $$\Pr(\mathfrak{G} \le \tilde{u}) = \exp\left(-e^{-2\tilde{u}}\right).$$

Formula (7.12) is an asymptotic equality in distribution, and the distribution of $\mathfrak{G}$ is a so-called Gumbel (or double exponential) distribution of the sort that arises in extreme value theory [44].

It should be pointed out that formula (7.12) has a direct physical interpretation. If a is taken to equal $C\epsilon^{-1/2}$ for some $C > 0$, so that $\mathfrak{u}$ is the amount of time that elapses between the moment the final approach path reaches $x^1 = C$ and the moment of final absorption at $x^1 = 0$, formula (7.12) implies that to leading order as $\epsilon \to 0$,

(7.14) $$E\mathfrak{u} \sim \log\left(C\epsilon^{-1/2}\right) \sim (1/2)\log(\epsilon^{-1})$$

irrespective of C. In other words, the time needed for the process to make its final approach to the characteristic boundary grows logarithmically in ϵ. This logarithmic growth is to be contrasted with the *exponential* growth of the MFPT $E\tau_\epsilon$ as $\epsilon \to 0$. The exponential timescale is the timescale on which a successful exit is expected to occur; when it occurs, however, it takes place on a much faster (logarithmic) timescale. This is the timescale of the 'Great Leap Forward' of Ludwig [30]; see also Refs. [32, 34]. Actually, formula (7.12) permits a refinement of Ludwig's picture. $(1/2)\log(\epsilon^{-1})$ is essentially the time needed for the deterministic MPEP to approach within an $\mathcal{O}(\epsilon^{1/2})$ distance of the characteristic boundary. On that lengthscale (the width of the boundary layer) the MPEP ceases to be well-defined; equivalently, the limiting approach path process ceases to be deterministic. The Gumbel random variable $\mathfrak{G}$ of (7.12) is the extra, random, amount of time needed for the process to reach the boundary.

We now consider the the implications of the representation (7.12) for the time-reversed process $\tilde{X}(u)$, $u \geq 0$, and the weighted integral $\mathfrak{I}(\mu)$. $\tilde{X}$ is an Ornstein-Uhlenbeck process satisfying

$$d\tilde{X}(u) = -\tilde{X}(u)\,du + dw(u), \tag{7.15}$$

conditioned to satisfy $\tilde{X}(0) = 0$ and $\tilde{X}(u) > 0$ for all $u > 0$. Moreover, it is conditioned to satisfy $\tilde{X}(\mathfrak{u}) = a$. In the large-$a$ limit we may write this condition as $\tilde{X}(\log a + \mathfrak{G}) = a$, and conditioning on the event $\mathfrak{G} = \tilde{u}$ will impose an extra condition

$$\tilde{X}(\log a + \tilde{u}) = a \tag{7.16}$$

on the process $\tilde{X}$. In the language of random processes, once a value $\tilde{u}$ for the Gumbel random variable $\mathfrak{G}$ is specified, the process $\tilde{X}(u)$, $u \geq 0$, becomes a *conditioned Ornstein-Uhlenbeck meander process*. 'Meander' refers to the fact that $\tilde{X}(u) > 0$ for all $u > 0$, *i.e.*, the fact that return to zero (*i.e.*, to $\partial\Omega$) is not allowed [16].

We shall shortly see that imposing the condition (7.16) on an Ornstein-Uhlenbeck meander process, and taking the $a \to \infty$ limit, yields a well-defined process which we may denote $\tilde{X}_{\tilde{u}}(u)$, $u \geq 0$. This being the case, define

$$\mathfrak{I}_{\tilde{u}}(\mu) = \int_0^\infty e^{-\mu u}\tilde{X}_{\tilde{u}}(u)\,du \tag{7.17}$$

to be the conditioned version of $\mathfrak{I}(\mu)$. By (7.6) the moments of $\mathfrak{S}_\epsilon/\epsilon^{1/2}$, the normalized displacement along $\partial\Omega$ at the time of hitting, satisfy

$$\begin{aligned} E(\mathfrak{S}_\epsilon/\epsilon^{1/2})^k &\sim \sum_{l=0}^{k}\binom{k}{l}c^l(2\mu)^{-(k-l)/2}\ E\,\mathfrak{I}(\mu)^l\ \ E\,\mathfrak{Z}^{k-l} \\ &= \sum_{l=0}^{k}\binom{k}{l}c^l(2\mu)^{-(k-l)/2}[(k-l)!!]\ E\,\mathfrak{I}(\mu)^l \\ &= \sum_{l=0}^{k}\binom{k}{l}c^l(2\mu)^{-(k-l)/2}[(k-l)!!]\int_{\tilde{u}=0}^{\infty} E\mathfrak{I}_{\tilde{u}}(\mu)^l\,d[\exp(-e^{-2\tilde{u}})] \end{aligned} \tag{7.18}$$

where the integral arises from removing the conditioning $\mathfrak{G} = \tilde{u}$. This formula is the key result of this section: It expresses the moments of the asymptotic exit location distribution $p_\epsilon(s)\,ds$, when $\mu > 1$, in terms of those of the random variables $\mathfrak{I}_{\tilde{u}}(\mu)$. We now explain how to compute the moments of the $\mathfrak{I}_{\tilde{u}}(\mu)$.

For any specified $\tilde{u}$, $\tilde{X}_{\tilde{u}}(u)$, $u \ge 0$, is a Markov process whose transition probabilities may be computed by taking the above $a \to \infty$ limit. However, it turns out to be time-inhomogeneous. To simplify the moment computations, it is preferable to express $\mathfrak{I}_{\tilde{u}}(\mu)$ in terms of a related time-homogeneous process, which is based on Brownian rather than Ornstein-Uhlenbeck motion. This process, which we shall call $w_{\tilde{u}}^{+}(t)$, $t \ge 0$, is introduced as follows. Recall that a standard Ornstein-Uhlenbeck process $o(u)$, $u \ge 0$ satisfies

$$o(u) = e^{-u} w\left((e^{2u} - 1)/2\right) \tag{7.19}$$

in the sense of equality in distribution; here $w(t)$, $t \ge 0$, is a standard Wiener process. Formally, imposing the condition $o(u) > 0$ for all $u > 0$ is equivalent to imposing the condition $w(t) > 0$ for all $t > 0$. So Ornstein-Uhlenbeck meander o^{+} and Brownian meander w^{+} are also related by

$$o^{+}(u) = e^{-u} w^{+}\left((e^{2u} - 1)/2\right). \tag{7.20}$$

Accordingly, imposing the condition $o^{+}(u) = a$ on Ornstein-Uhlenbeck meander o^{+} at time $u = \log a + \tilde{u}$ is equivalent to imposing the condition

$$a = e^{-u} w^{+}\left((e^{2u} - 1)/2\right) \tag{7.21}$$

at time $u = \log a + \tilde{u}$ on the associated Brownian meander w^{+}, *i.e.*, imposing the condition $w^{+}\left([a^2 e^{2\tilde{u}} - 1]/2\right) = a^2 e^{\tilde{u}}$. By defining $T = a^2 e^{2\tilde{u}}/2$, we see that for any fixed $\tilde{u}$, in the large-a (*i.e.*, large-T) limit this condition is to leading order a requirement that

$$w^{+}(T) = 2e^{-\tilde{u}} T. \tag{7.22}$$

In other words, imposing the condition $o^{+}(u) = a$ on Ornstein-Uhlenbeck meander, when $u = \log a + \tilde{u}$, in the large-a limit forces the associated Brownian meander to *drift outward* at a mean speed $2e^{-\tilde{u}}$.

We now define $w_{\tilde{u}}^{+}(t)$, $t \ge 0$, to be the weak limit as $T \to \infty$ (*i.e.*, as $a \to \infty$) of the standard Brownian meander process $w^{+}(t)$, $t \ge 0$, when constrained by the condition (7.22). We necessarily have, as an equality in distribution,

$$\tilde{X}_{\tilde{u}}(u) = e^{-u} w_{\tilde{u}}^{+}\left((e^{2u} - 1)/2\right), \tag{7.23}$$

so that

$$\begin{aligned} \mathfrak{I}_{\tilde{u}}(\mu) &= \int_0^\infty e^{-\mu u} \tilde{X}_{\tilde{u}}(u)\, du \\ &= \int_0^\infty e^{-(\mu+1)u} w_{\tilde{u}}^{+}\left((e^{2u} - 1)/2\right) du \\ &= \int_0^\infty (1 + 2t)^{-(\mu+3)/2} w_{\tilde{u}}^{+}(t)\, dt. \end{aligned} \tag{7.24}$$

The last equality follows by a change of variables $t = (e^{2u} - 1)/2$. The formula (7.24) permits the computation of the moments of $\mathfrak{I}_{\tilde{u}}(\mu)$, as required by (7.18), from the correlation functions (*i.e.*, finite-dimensional distributions) of the process $w_{\tilde{u}}^{+}$. We shall shortly see that $w_{\tilde{u}}^{+}$ is time-homogeneous, making this representation particularly useful.

The n-point correlation functions of $w_{\tilde{u}}^{+}$ may be computed by taking the $T \to \infty$ limit of the n-point correlation functions of Brownian meander w^{+}, conditioned by (7.22). The evaluation of this limit is facilitated by the following fact. Recall that a *three-dimensional*

Bessel process $B(t)$, $t \geq 0$, is the radial coordinate in $\mathbb{R}^3$ of a diffusing particle, conventionally taken to satisfy $B(0) = 0$. That is, $B(t)$ equals $[w_1^2(t) + w_2^2(t) + w_3^2(t)]^{1/2}$, where the $w_i(t)$ are independent standard Wiener processes. It is a useful result [25] that the Bessel process B, when conditioned to satisfy $B(t') = x'$ for any specified $t' > 0$ and $x' > 0$, and Brownian meander w^+, when conditioned to satisfy $w^+(t') = x'$, become identical in distribution on the time interval $0 \leq t \leq t'$. This allows us to substitute the Bessel process for Brownian meander, and to compute instead the $T \to \infty$ limit of the n-point correlation functions of B, conditioned on $B(T) = 2e^{-\tilde{u}}T$. The substitution of B for w^+ simplifies the computation, for the Bessel process is (unlike Brownian meander) time-homogeneous.

Denote by $q(w_1, t_1; w_2, t_2)$ the transition density of the standard Wiener process, *i.e.*,

$$q(w_1, t_1; w_2, t_2) \stackrel{\text{def}}{=} [2\pi(t_2 - t_1)]^{-1/2} \exp\left[-(w_2 - w_1)^2/2(t_2 - t_1)\right]. \tag{7.25}$$

If instants $0 < t_1 < \ldots < t_n$ are specified, the n-point correlation function of the Bessel process B, which we shall denote $p^{(n)}(\cdot, t_1; \ldots; \cdot, t_n)$, is defined by

$$p^{(n)}(w_1, t_1; \ldots; w_n, t_n) \stackrel{\text{def}}{=} \Pr\left(B(t_i) \in w_i + dw_i,\ 1 \leq i \leq n\right) \Big/ \prod_{i=1}^{n} dw_i\ . \tag{7.26}$$

It satisfies

$$p^{(n)}(w_1, t_1; \ldots; w_n, t_n) = p^{(1)}(w_1, t_1) \prod_{i=1}^{n-1} t(w_i, t_i; w_{i+1}, t_{i+1}) \tag{7.27}$$

where

$$p^{(1)}(w_1, t_1) = \sqrt{\frac{2}{\pi t_1^3}} w_1^2 \exp\left(-w_1^2/2t_1\right) \tag{7.28}$$

and

$$t(w_1, t_1; w_2, t_2) = (w_2/w_1)\left[q(w_1, t_1; w_2, t_2) - q(-w_1, t_1; w_2, t_2)\right] \tag{7.29}$$

are the probability density and transition density for the Bessel process. Conditioning on the event $B(T) = 2e^{-\tilde{u}}T$, where $T > t_n$, yields a process with n-point correlation function

$$p^{(n)}_{\tilde{u},T}(w_1, t_1; \ldots; w_n, t_n) \stackrel{\text{def}}{=} \frac{p^{(n+1)}(w_1, t_1; \ldots; w_n, t_n; 2e^{-\tilde{u}}T, T)}{p^{(1)}(2e^{-\tilde{u}}T, T)}. \tag{7.30}$$

In particular, the conditioned density $p^{(1)}_{\tilde{u},T}(w_1, t_1)$ satisfies

$$p^{(1)}_{\tilde{u},T}(w_1, t_1) = p^{(1)}(w_1, t_1)\left[\frac{t(w_1, t_1; 2e^{-\tilde{u}}T, T)}{p^{(1)}(2e^{-\tilde{u}}T, T)}\right], \tag{7.31}$$

and the conditioned transition density $t_{\tilde{u},T}(w_1, t_1; w_2, t_2)$ satisfies

$$t_{\tilde{u},T}(w_1, t_1; w_2, t_2) = \frac{p^{(2)}_{\tilde{u},T}(w_1, t_1; w_2, t_2)}{p^{(1)}_{\tilde{u},T}(w_1, t_1)} = t(w_1, t_1; w_2, t_2)\left[\frac{t(w_2, t_2; 2e^{-\tilde{u}}T, T)}{t(w_1, t_1; 2e^{-\tilde{u}}T, T)}\right]. \tag{7.32}$$

Let $\tilde{p}^{(1)}_{\tilde{u}}(w_1,t_1)$ and $\tilde{t}_{\tilde{u}}(w_1,t_1;w_2,t_2)$ be the $T\to\infty$ limits of $p^{(1)}_{\tilde{u},T}(w_1,t_1)$ and $t_{\tilde{u},T}(w_1,t_1;w_2,t_2)$ respectively. It follows by taking the $T\to\infty$ limit of the two factors in brackets that

$$\begin{aligned}\tilde{p}^{(1)}_{\tilde{u}}(w_1,t_1) &= p^{(1)}(w_1,t_1)e^{-v^2t_1/2}\left(\frac{\sinh vw_1}{vw_1}\right)\\ &= \frac{1}{\sqrt{2\pi t_1^3}}(w_1/v)\left[e^{-(w_1-vt_1)^2/2t_1}-e^{-(w_1+vt_1)^2/2t_1}\right]\end{aligned} \tag{7.33}$$

and

$$\begin{aligned}&\tilde{t}_{\tilde{u}}(w_1,t_1;w_2,t_2) =\\ &e^{-v^2(t_2-t_1)/2}\left(\frac{\sinh vw_2}{\sinh vw_1}\right)\left[q(w_1,t_1;w_2,t_2)-q(-w_1,t_1;w_2,t_2)\right].\end{aligned} \tag{7.34}$$

Here $v \stackrel{\text{def}}{=} 2e^{-\tilde{u}}$ is the quantity referred to above as a mean outward drift speed. $\tilde{p}^{(1)}_{\tilde{u}}(w_1,t_1)$ and $\tilde{t}_{\tilde{u}}(w_1,t_1;w_2,t_2)$ are the density and transition density of the limiting process $w^+_{\tilde{u}}(t)$, $t\geq 0$.

The transition density $\tilde{t}_{\tilde{u}}(w_1,t_1;w_2,t_2)$ is invariant under time translation, so the limiting process is a time-homogeneous Markov process as promised. It is well known [40], and also follows from the form of the transition density (7.29), that the three-dimensional Bessel process has generator $-(1/2)d^2/dw^2-(1/w)d/dw$. Similarly, it follows from the formula (7.34) for the transition density $\tilde{t}_{\tilde{u}}(w_1,t_1;w_2,t_2)$ that the process $w^+_{\tilde{u}}(t)$, $t\geq 0$, has generator $-(1/2)d^2/dw^2-(v\coth vw)d/dw$. The coefficient $v\coth vw$ is asymptotic to $1/w$ as $w\to 0$, and to v as $w\to\infty$. This confirms that $v=2e^{-\tilde{u}}$ can be viewed as the speed of a superimposed outward drift.

Now that the probability density and transition density of the process $w^+_{\tilde{u}}$ are known, its n-point correlation functions $p^{(n)}_{\tilde{u}}(w_1,t_1;\ldots;w_n,t_n)$ follow from

$$\tilde{p}^{(n)}_{\tilde{u}}(w_1,t_1;\ldots;w_n,t_n) = \tilde{p}^{(1)}_{\tilde{u}}(w_1,t_1)\prod_{i=1}^{n-1}\tilde{t}_{\tilde{u}}(w_i,t_i;w_{i+1},t_{i+1}). \tag{7.35}$$

And since $\mathfrak{I}_{\tilde{u}}(\mu)$ is by (7.24) a weighted area under the process $w^+_{\tilde{u}}$, its moments can be expressed in terms of these n-point correlation functions by repeated integration. It is not clear, however, whether a closed-form expression for the distribution of $\mathfrak{I}_{\tilde{u}}(\mu)$ exists. If it does it is likely to be quite intricate, as is suggested by the results of other authors. The problem of computing the distribution of the (unweighted) area under a Brownian bridge (*i.e.*, a pinned Wiener process) was solved by Shepp [48] and others, and the corresponding problem for a Brownian excursion by Louchard [28]. More recently, Takács [49] has computed the distribution of the integral of the absolute value of a Wiener process. All these distributions have closed-form expressions that are surprisingly complicated; they involve, for example, double Laplace transforms of the logarithmic derivative of an Airy function.

It is unfortunate that one cannot go directly from (7.33) and (7.34), or from the explicit expression for the generator of the process $w^+_{\tilde{u}}$, to a closed-form expression for the distribution of $\mathfrak{I}_{\tilde{u}}(\mu)$. If such an expression were known, it would be possible to remove (by integration) the conditioning on $\mathfrak{G}=\tilde{u}$, and obtain a closed-form expression for the distribution of $\mathfrak{I}(\mu)$. This in turn would yield a closed-form expression for the limiting exit location distribution on the $\mathcal{O}(\epsilon^{1/2})$ lengthscale. But in the absence of such an expression one can at least compute the moments of the limiting distribution to any desired order, by using (7.18), (7.24), (7.33), and (7.34).

The case of the first moment (the expected offset from the saddle point H along the boundary $\partial\Omega$, at the time $\partial\Omega$ is reached) is particularly straightforward. By (7.18),

$$E(\mathfrak{S}_\epsilon/\epsilon^{1/2}) \sim c\, E\, \mathfrak{I}(\mu) \tag{7.36}$$

where

$$E\mathfrak{I}(\mu) = \int_{\tilde{u}=0}^{\infty} E\, \mathfrak{I}_{\tilde{u}}(\mu)\, d[\exp(-e^{-2\tilde{u}})]. \tag{7.37}$$

Moreover, by (7.24)

$$E\mathfrak{I}_{\tilde{u}}(\mu) = \int_0^\infty (1+2t)^{-(\mu+3)/2}\, E\, w_{\tilde{u}}^{+}(t)\, dt, \tag{7.38}$$

in which

$$Ew_{\tilde{u}}^{+}(t) = \int_0^\infty w\, p_{\tilde{u}}^{(1)}(w,t)\, dw, \tag{7.39}$$

with the density $p_{\tilde{u}}^{(1)}(w,t)$ given by (7.33). Evaluating the integral (7.39) yields

$$Ew_{\tilde{u}}^{+}(t) = (v^{-1}+vt)\,\mathrm{erf}\left(\sqrt{v^2t/2}\right) + \sqrt{\frac{2t}{\pi}}e^{-v^2t/2}, \tag{7.40}$$

which is a result of independent interest; this quantity is the expected distance from $\partial\Omega$ (on the $\mathcal{O}(\epsilon^{1/2})$ lengthscale) at t time units before exit, if one conditions on the Gumbel random variable $\mathfrak{G}$ equalling $\tilde{u}$. Substitution of (7.40) into (7.38) and (7.37) yields, after various manipulations,

$$E\mathfrak{I}(\mu) = \sqrt{\frac{2}{\pi}}\frac{1}{\mu^2-1} + \frac{B(1/2,\mu/2)}{4\sqrt{\pi}(\mu-1)} \tag{7.41}$$

where $B(\cdot,\cdot)$ is the Euler beta function. We conclude, by (7.36), that the expected offset from the saddle point at the time of exit, *i.e.*, $E\mathfrak{S}_\epsilon = \int_0^\infty s\, p_\epsilon(s)\, ds$, is when $\mu > 1$ asymptotically equal to $c\epsilon^{1/2}$ times this function of the eigenvalue ratio μ.

This result on the first moment provides additional information on the degree of skewing present in generic $\mu > 1$ models, over and above the differing $s/\epsilon^{1/2} \to \pm\infty$ asymptotics of $p_\epsilon(s)$ given in (7.8). It is in fact possible to speculate, on the basis of the Gaussian falloff rates and the first moment, on the functional form of the generic asymptotic exit location distribution when $\mu > 1$. But we shall resist the temptation.

We note briefly, in conclusion, that the probabilistic analysis of this section may be extended to models with $\mu < 1$ as well. If $\mu < 1$, we showed in Section 4 that generically the MPEP is tangent to $\partial\Omega$. If the linearized drift $\boldsymbol{B}(H)$ is normalized as in (6.1), and $\boldsymbol{D}(H) = \boldsymbol{I}$, the MPEP approaches the saddle point $H = (0,0)$ along a curve $x^2 \sim A(x^1)^\mu$, where A can only be computed by integrating Hamilton's equations from S to H. In this case the conditioning on $x^1 = a\epsilon^{1/2}$ at time $t = \tau_\epsilon - \mathfrak{u}$ must be supplemented by a conditioning on $x^2 = A(a\epsilon^{1/2})^\mu$. It follows from the stochastic differential equation (7.2b) that asymptotically, $x_\epsilon^2(\tau_\epsilon) \sim x_\epsilon^2(\tau_\epsilon - \mathfrak{u})\exp(-\mu\mathfrak{u})$, irrespective of the value taken by the coefficient c. Since $\mathfrak{u} \sim \log a + \mathfrak{G}$, this implies that when $\mu < 1$,

$$\begin{aligned}\mathfrak{S}_\epsilon &\sim A(a\epsilon^{1/2})^\mu \exp[-\mu(\log a + \mathfrak{G})],\\ &= A\epsilon^{\mu/2}\exp(-\mu\mathfrak{G}).\end{aligned} \tag{7.42}$$

By examination, this offset random variable $\mathfrak{S}_\epsilon$ has the Weibull distribution (6.16) previously computed by the method of matched asymptotic expansions! This alternative derivation makes it clear how the Weibull distribution on the $\mathcal{O}(\epsilon^{\mu/2})$ lengthscale, when $\mu < 1$, arises from the underlying stochastics; in particular, from the Gumbel distribution of the 'extra time to absorption' random variable $\mathfrak{G}$.

8. Two-dimensional Ackerberg-O'Malley resonance. Now that we have to a large extent determined the generic asymptotic exit location distributions, in this section we digress to discuss the interplay between our results and a well known singularly perturbed boundary value problem. Recall that if

$$\mathcal{L}_\epsilon = -(\epsilon/2)D^{ij}\partial_i\partial_j - b^i\partial_i \tag{8.1}$$

is the generator of the process $\boldsymbol{x}_\epsilon(t)$, $t \geq 0$, then the solution u_ϵ of the boundary value problem

$$\mathcal{L}_\epsilon u_\epsilon = \lambda u_\epsilon \text{ in } \Omega,\, u_\epsilon = f \text{ on } \partial\Omega \tag{8.2}$$

will in the special case $\lambda = 0$ satisfy

$$u_\epsilon(\boldsymbol{y}) = E_{\boldsymbol{y}} f(\boldsymbol{x}_\epsilon(\tau_\epsilon)) \tag{8.3}$$

where the subscript on E signifies the starting point $\boldsymbol{x}_\epsilon(0)$ for the process. As $\epsilon \to 0$ the function u_ϵ is expected to 'level,' or tend to a constant, exponentially rapidly; this has been verified rigorously for the case of a non-characteristic boundary by Eizenberg [18]. The levelling meshes with the probabilistic picture that for any $\boldsymbol{y} \in \Omega$, as $\epsilon \to 0$ it becomes overwhelmingly (exponentially) likely that a sample path for the process $\boldsymbol{x}_\epsilon(t)$ will first flow toward the stable point S, and approach S to within an $\mathcal{O}(\epsilon^{1/2})$ distance, before experiencing further fluctuations. As a consequence the expectation $E_{\boldsymbol{y}}$ in (8.3) may up to exponentially small relative errors be replaced by E_S, and $u_\epsilon(\boldsymbol{y})$ may be approximated by a $\boldsymbol{y}$-independent constant. If we assume the exit location on $\partial\Omega$ converges in probability to a saddle point H as $\epsilon \to 0$, and that f is continuous at H, then $u_\epsilon(\boldsymbol{y}) \to f(H)$ for all $\boldsymbol{y} \in \Omega$.

Even though u_ϵ will level exponentially rapidly and may be approximated by a constant, the constant itself may converge comparatively slowly to $f(H)$ as $\epsilon \to 0$. It is possible to apply our results to determine its asymptotics, and the speed of its convergence to $f(H)$, as $\epsilon \to 0$. The basic idea is due to Matkowsky, Schuss, and Tier [39]. The results we need are (6.17) and (7.41), which give the expected offset from H along $\partial\Omega$, at the time the process $\boldsymbol{x}_\epsilon(t)$ exits Ω. In the standardization of the last two sections (the unstable eigenvalue $\lambda_u(H)$ taken to equal unity, and $\boldsymbol{D}(H)$ taken to equal $\boldsymbol{I}$), we found that the expected offset $E\mathfrak{S}_\epsilon = \int_0^\infty s\, p_\epsilon(s)\, ds$ has asymptotics

$$E\mathfrak{S}_\epsilon \sim [A\Gamma(1+\mu/2)]\,\epsilon^{\mu/2}, \quad \epsilon \to 0 \tag{8.4}$$

if $\mu < 1$, *i.e.*, $\partial_i b^i(H) > 0$, and

$$E\mathfrak{S}_\epsilon \sim c\left[\sqrt{\frac{2}{\pi}}\frac{1}{\mu^2-1} + \frac{B(1/2,\mu/2)}{4\sqrt{\pi}(\mu-1)}\right]\epsilon^{1/2}, \quad \epsilon \to 0 \tag{8.5}$$

if $\mu > 1$, *i.e.*, $\partial_i b^i(H) < 0$. Here $\mu = |\lambda_s(H)|/\lambda_u(H)$ as always, A is a quantity that may be computed from the way in which the generically unique Wentzell-Freidlin trajectory from S to H (the MPEP) approaches H, and c is the off-diagonal element of the linearization of $\boldsymbol{b}$ at H (see (6.1) and (7.1)). $B(\cdot,\cdot)$ is the Euler beta function.

It follows from (8.3), (8.4), and (8.5) that if f on $\partial\Omega$ is continuously differentiable at H, then for all $\boldsymbol{y} \in \Omega$, $u_\epsilon(\boldsymbol{y})$ has leading $\epsilon \to 0$ asymptotics

$$u_\epsilon(\boldsymbol{y}) \sim \begin{cases} f(H) + [A\Gamma(1+\mu/2)]\, f'(H)\epsilon^{\mu/2}, & \text{if } \mu < 1; \\ f(H) + c\left[\sqrt{\frac{2}{\pi}}\frac{1}{\mu^2-1} + \frac{B(1/2,\mu/2)}{4\sqrt{\pi}(\mu-1)}\right] f'(H)\epsilon^{1/2}, & \text{if } \mu > 1, \end{cases} \tag{8.6}$$

which are independent of $\boldsymbol{y}$. If $\mu > 1$ and $c = 0$ (a *local gradient* condition at H, as discussed in Section 5) then the $\mathcal{O}(\epsilon^{1/2})$ correction to $f(H)$ will have zero coefficient. The same will occur, irrespective of μ, if $b^i = -D^{ij}\Phi_{,j}$, *i.e.*, if the drift field $\boldsymbol{b}$ is globally gradient. In these nongeneric cases the asymptotic exit location distribution will be a Gaussian centered on H, on the $\mathcal{O}(\epsilon^{1/2})$ lengthscale, and the leading correction to $f(H)$ in u_ϵ will necessarily be $\mathcal{O}(\epsilon^{1/2})$.

The asymptotics of (8.6) are striking, especially in the case $\mu < 1$. Since μ need not be rational, the presence of a leading correction term proportional to $\epsilon^{\mu/2}$ implies that u_ϵ *on* Ω *cannot in general be expanded in an asymptotic series in integral powers of* ϵ*, or even in fractional powers*. To place this result in context, we remind the reader that the analogue for one-dimensional problems of the phenomenon we are investigating (the existence of a nontrivial $\epsilon \to 0$ limit on Ω for the solution u_ϵ of the singularly perturbed boundary value problem (8.2), for certain values of λ) is known as *Ackerberg-O'Malley resonance* [1]. In the one-dimensional case the partial differential equation $\mathcal{L}_\epsilon u_\epsilon = \lambda u_\epsilon$ reduces to an ordinary differential equation. One may solve for u_ϵ in closed form [43]. It is not difficult to show that when $\lambda = 0$, u_ϵ both levels and converges exponentially rapidly. The exponential levelling, and the constant limit, have the same interpretation in terms of the stochastic exit problem as they do in two-dimensional models.

The presence of irrational powers of ϵ in the outer expansion for u_ϵ, in two-dimensional resonance, suggests that they may also be present in the outer expansion for the principal eigenfunction v_ϵ^0 of $\mathcal{L}_\epsilon^*$ (the quasistationary density). That is the reason why, unlike many authors, we have refrained in this paper from approximating the quasistationary density in the body of Ω by a formal asymptotic series, since it is unclear what powers of ϵ should be present. Instead, we have worked only to leading order. As we noted at the beginning of Section 3, for an outer expansion to be useful it must match to an inner expansion. And the expansion beyond leading order of the quasistationary density v_ϵ^0 in the boundary layer remains an unsolved problem.

9. Conclusions. The generic features of the two-dimensional stochastic exit problem with characteristic boundary, when exit from the region Ω occurs over a saddle H, are now clear. As the noise strength $\epsilon \to 0$, the distribution of exit points on the separatrix will be concentrated on the $\mathcal{O}(\epsilon^{\mu/2})$ lengthscale near H (if the eigenvalue ratio $\mu < 1$) or the $\mathcal{O}(\epsilon^{1/2})$ lengthscale (if $\mu > 1$). In the $\mu < 1$ case the exit location distribution is asymptotic to the Weibull distribution (6.16), which includes a scale factor that can only be computed from the approach path taken by the MPEP (the optimal, or most probable trajectory) from S to H. In the $\mu > 1$ case the limiting exit location distribution, whose moments are computable (see, *e.g.*, (7.41)), contains no free parameters: it is determined by the stochastic dynamics in the vicinity of H.

In both cases the limiting distribution will be 'skewed': non-Gaussian and asymmetric. Normally, it is Gaussian only when the deterministic drift $\boldsymbol{b}$ satisfies $b^i = -D^{ij}\partial_j\Phi$ for some potential function Φ, or when $\mu > 1$ and a local version of this equality (the $c = 0$ condition of Section 5) holds near H. These cases, which are characterized by the absence of a classically forbidden 'wedge' emanating from H, are nongeneric. Although our two-dimensional stochastic model differs from the barrier crossing models employed in chemical physics, we believe that the genericity of the skewing phenomenon is related to the phenomenon of 'saddle point avoidance' [2, 4]. A number of authors have in fact already noted the presence (in particular models) of a classically forbidden region. In the literature the boundary of the forbidden region is sometimes called the 'stochastic separatrix' [2, 4, 17, 24, 42].

It is clear from our treatment that the generic features of models with $\mu < 1$ are particularly interesting. In such models the frequency factor $K(H)$ (the value of the WKB prefactor at $\boldsymbol{x} = H$, which would normally be interpreted as a factor by which the frequency of excursions to the vicinity of H is multiplied) equals *zero*. This feature, like the anomalously large lengthscale over which the exit location distribution is spread [$\mathcal{O}(\epsilon^{\mu/2})$ rather than $\mathcal{O}(\epsilon^{1/2})$] can be traced to the unusual approach path taken by the MPEP. When $\mu < 1$ the MPEP is generically tangent to the separatrix $\partial\Omega$ at H, as in Fig. 4.1(a). This grazing behavior causes the exit location distribution to be anomalously wide. It also causes the WKB prefactor $K(\boldsymbol{x})$ to tend to zero as $\boldsymbol{x} \to H$ along the MPEP, as can be shown by integrating the system of ordinary differential equations (3.8a), (3.8b), (3.11), (3.12), (3.14) from S to H. Another unusual feature of generic models with $\mu < 1$ is that the traditional ('Eyring') formula (5.24) for the mean exit time asymptotics must be replaced by (6.19). The formula (6.19) is unaffected by $K(H)$ equalling zero, and by the fact that generically, the Hessian matrix of the Wentzell-Freidlin action W does not exist at H.

In this paper we have only begun the exploration of the geometric aspects of the exit problem. We commented briefly on the interpretation of the matrix Riccati equation (3.14) for $\partial_i\partial_j W$ in terms of symplectic geometry. The transport equation (3.12) for $K(\cdot)$ also has a geometric interpretation [15, 38]. The natural setting for the outer approximation $K(\boldsymbol{x})\exp\left(-W(\boldsymbol{x})/\epsilon\right)$ is the theory of semiclassical expansions for partial differential equations, which has deep geometric underpinnings.

It should be possible to extend our analysis in several directions. It has recently become clear that caustics (folds in the Lagrangian manifold $\mathcal{M}^u_{(S,0)}$ in phase space comprising the most probable fluctuational trajectories, as in Section 3) occur very frequently [17, 33]. Their effect on exit phenomena is now under investigation [35]. A second extension, of particular value in applications, would be to the case of degenerate diffusion. The results of this paper apply to what is known in physics as the *overdamped limit* of barrier crossing models. The analysis of exit location distributions in models with underdamped dynamics will require an extension to the case when the diffusion tensor is allowed to become singular [42].

Perhaps the most interesting extension would be to place our approach in the context of the singular perturbation theory of general partial differential equations. The phenomenon of skewing near a saddle point, as displayed in the asymptotic solution of the forward Kolmogorov equation, may simply be a special case of a more general phenomenon.

REFERENCES

[1] R. C. ACKERBERG AND R. E. O'MALLEY, JR., *Boundary layer problems exhibiting resonance*, Stud. Appl. Math., 49 (1970), pp. 277–295.

[2] N. AGMON AND R. KOSLOFF, *Dynamics of two-dimensional barrier crossing*, J. Phys. Chem., 91 (1987), pp. 1988–1996.

[3] R. E. BARLOW AND F. PROSCHAN, *Statistical Theory of Reliability and Life Testing*, Holt, Rinehart and Winston, New York, 1975.

[4] A. M. BEREZHKOVSKII, L. M. BEREZHKOVSKII, AND V. Y. ZITSERMAN, *The rate constant in the Kramers multidimensional theory and the saddle point avoidance*, Chem. Phys., 130 (1989), pp. 55–63.

[5] S. BITTANTI, A. J. LAUB, AND J. C. WILLEMS, eds., *The Riccati Equation*, Springer-Verlag, New York/Berlin, 1991.

[6] B.-Z. BOBROVSKY AND Z. SCHUSS, *A singular perturbation approach for the computation of the mean first passage time in a nonlinear filter*, SIAM J. Appl. Math., 42 (1982), pp. 174–187.

[7] B.-Z. BOBROVSKY AND O. ZEITOUNI, *Some results on the problem of exit from a domain*, Stochastic Process. Appl., 41 (1992), pp. 241–256.

[8] B. CARMELI, V. MUJICA, AND A. NITZAN, *Dynamics of multidimensional barrier crossing in the overdamped limit*, Berichte der Bunsen-Gesellschaft, 95 (1991), pp. 319–326.

[9] M. V. DAY, *Recent progress on the small parameter exit problem*, Stochastics, 20 (1987), pp. 121–150.

[10] ———, *Large deviations results for the exit problem with characteristic boundary*, J. Math. Anal. Appl., 147 (1990), pp. 134–153.

[11] ———, *Some phenomena of the characteristic boundary problem*, in Diffusion Processes and Related Problems in Analysis, M. Pinsky, ed., vol. 1, Birkhäuser, Boston/Basel, 1990, pp. 55–71.

[12] ———, *Cycling and skewing of exit measures for planar systems*, Stochastics, 48 (1994), pp. 227–247.

[13] ———, *Regularity of boundary quasipotentials for planar systems*, Appl. Math. Optim., 30 (1994), pp. 79–101.

[14] M. V. DAY AND T. A. DARDEN, *Some regularity results on the Ventcel–Freidlin quasi-potential function*, Appl. Math. Optim., 13 (1985), pp. 259–282.

[15] J. J. DUISTERMAAT, *Oscillatory integrals, Lagrange immersions, and unfolding of singularities*, Comm. Pure Appl. Math., 27 (1974), pp. 207–281.

[16] R. T. DURRETT, D. L. IGLEHART, AND D. R. MILLER, *Weak convergence to Brownian meander and Brownian excursion*, Ann. Probab., 5 (1977), pp. 117–129.

[17] M. I. DYKMAN, M. M. MILLONAS, AND V. N. SMELYANSKIY, *Observable and hidden singular features of large fluctuations in nonequilibrium systems*, Phys. Lett. A, 195 (1994), pp. 53–58. Available as cond-mat/9410056.

[18] A. EIZENBERG, *The exponential leveling and the Ventcel–Freidlin "minimal action" function*, J. Analyse Math., 54 (1990), pp. 99–111.

[19] A. EIZENBERG AND Y. KIFER, *The asymptotic behavior of the principal eigenvalue in a singular perturbation problem with invariant boundaries*, Probab. Theory Related Fields, 76 (1987), pp. 439–476.

[20] M. I. FREIDLIN AND A. D. WENTZELL, *Random Perturbations of Dynamical Systems*, Springer-Verlag, New York/Berlin, 1984.

[21] S. GLASSTONE, K. J. LAIDLER, AND H. EYRING, *The Theory of Rate Processes*, McGraw-Hill, New York, 1941.

[22] H. R. JAUSLIN, *Nondifferentiable potentials for nonequilibrium steady states*, Physica A, 144 (1987), pp. 179–191.

[23] Y. KIFER, *On the principal eigenvalue in a singular perturbation problem with hyperbolic limit points and circles*, J. Differential Equations, 37 (1980), pp. 108–139.

[24] M. M. KŁOSEK-DYGAS, B. M. HOFFMAN, B. J. MATKOWSKY, A. NITZAN, M. A. RATNER, AND Z. SCHUSS, *Diffusion theory of multidimensional activated rate processes: The role of anisotropy*, J. Chem. Phys., 90 (1989), pp. 1141–1148.

[25] F. B. KNIGHT, *On the excursion process of Brownian motion*, Trans. Amer. Math. Soc., 258 (1980), pp. 77–86.

[26] P. LANCASTER AND L. RODMAN, *Solutions of the continuous and discrete time algebraic Riccati equations: A review*, in Bittanti et al. [5], pp. 11–51.

[27] R. LANDAUER AND J. A. SWANSON, *Frequency factors in the thermally activated process*, Phys. Rev., 121 (1961), pp. 1668–1674.

[28] G. LOUCHARD, *Kac's formula, Levy's local time and Brownian excursion*, J. Appl. Probab., 21 (1984), pp. 479–499.

[29] D. LUDWIG, *Persistence of dynamical systems under random perturbations*, SIAM Rev., 17 (1975), pp. 605–640.

[30] ———, *Escape from domains of attraction for systems perturbed by noise*, in Nonlinear Phenomena in Physics and Biology, R. H. Enns, B. L. Jones, R. M. Miura, and S. S. Rangnekar, eds., Plenum Press, New York, 1981, pp. 549–566.

[31] R. S. MAIER, *Large fluctuations in stochastically perturbed nonlinear systems: Applications in computing*, in 1992 Lectures on Complex Systems, L. Nadel and D. L. Stein, eds., Addison-Wesley, New York, 1993, pp. 501–517. Proceedings of the 1992 Complex Systems Summer School (Santa Fé, June 1992).

[32] R. S. MAIER AND D. L. STEIN, *Transition-rate theory for non-gradient drift fields*, Phys. Rev. Lett., 69 (1992), pp. 3691–3695.

[33] ———, *The effect of focusing and caustics on exit phenomena in systems lacking detailed balance*, Phys. Rev. Lett., 71 (1993), pp. 1783–1786. Available as chao-dyn/9305010.

[34] ———, *The escape problem for irreversible systems*, Phys. Rev. E, 48 (1993), pp. 931–938. Available as chao-dyn/9303017.

[35] R. S. MAIER AND D. L. STEIN, *A scaling theory of bifurcations in the symmetric weak-noise escape problem*, J. Statist. Phys., 83 (1996), pp. 291–357.

[36] M. MANGEL, *Barrier transitions driven by fluctuations, with applications to evolution and ecology*, Theoret. Population Biol., 45 (1994), pp. 16–40.

[37] M. MANGEL AND D. LUDWIG, *Probability of extinction in a stochastic competition*, SIAM J. Appl. Math., 33 (1977), pp. 256–266.
[38] V. P. MASLOV AND M. V. FEDORIUK, *Semi-Classical Approximation in Quantum Mechanics*, Reidel, Boston/Dordrecht, 1981.
[39] B. J. MATKOWSKY, Z. SCHUSS, AND C. TIER, *Diffusion across characteristic boundaries with critical points*, SIAM J. Appl. Math., 43 (1983), pp. 673–695.
[40] H. P. MCKEAN, JR., *Excursions of a non-singular diffusion*, Z. Wahrsch. verw. Gebiete, 1 (1963), pp. 230–239.
[41] F. MOSS AND P. V. E. MCCLINTOCK, eds., *Theory of Noise-Induced Processes in Special Applications*, vol. 2 of Noise in Nonlinear Dynamical Systems, Cambridge University Press, Cambridge, 1989.
[42] T. NAEH, M. M. KŁOSEK, B. J. MATKOWSKY, AND Z. SCHUSS, *A direct approach to the exit problem*, SIAM J. Appl. Math., 50 (1990), pp. 595–627.
[43] R. E. O'MALLEY, JR., *Singular Perturbation Methods for Ordinary Differential Equations*, vol. 89 of Applied Mathematical Sciences, Springer-Verlag, New York/Berlin, 1991.
[44] S. I. RESNICK, *Extreme Values, Regular Variation, and Point Processes*, Springer-Verlag, New York/Berlin, 1987.
[45] D. RYTER AND B.-Z. BOBROVSKY, *On the distribution of exit points of randomly perturbed dynamical systems*, Tech. Report IKT-NT 1001, ETH-Zürich Comm. Technol. Lab, Zürich, 1991. Cited in Ref. [7].
[46] Z. SCHUSS, *Theory and Application of Stochastic Differential Equations*, Wiley, New York, 1980.
[47] M. A. SHAYMAN, *A geometric view of the matrix Riccati equation*, in Bittanti et al. [5], pp. 89–112.
[48] L. A. SHEPP, *On the integral of the absolute value of the pinned Wiener process*, Ann. Probab., 10 (1982), pp. 234–239.
[49] L. TAKÁCS, *On the distribution of the integral of the absolute value of the Brownian motion*, Adv. in Appl. Probab., 3 (1993), pp. 186–197.
[50] P. TALKNER, *Mean first passage times and the lifetime of a metastable state*, Z. Phys. B, 68 (1987), pp. 201–207.
[51] N. G. VAN KAMPEN, *Stochastic Processes in Physics and Chemistry*, North-Holland, New York/Amsterdam, 1981.
[52] A. WEISS, *A new technique for analysing large traffic systems*, Adv. in Appl. Probab., 18 (1986), pp. 506–532.
[53] A. L. WELTI AND B.-Z. BOBROVSKY, *Mean time to lose lock for a coherent second-order PN-code tracking loop – The singular perturbation theory approach*, IEEE Trans. Sel. Areas Comm., 8 (1990), pp. 809–818.